Influencing the macro- and microcirculatory complications of nonocclusive mesenteric ischemia by complement C5a inhibitor treatments

Miklós Nógrády M.D.

Ph.D. Thesis

University of Szeged,
Institute of Surgical Research
Doctoral School of Multidisciplinary Medical Sciences

Supervisors:
Gabriella Varga, PhD
Dániel Érces MD, PhD

2016

LIST OF PAPERS RELATED TO THE SUBJECT OF THE THESIS

List of full papers

I.   Vass A, Süveges G, Érces D, **Nógrády M**, Varga G, Földesi I, Futakuchi M, Imai M, Okada N, Okada H, Boros M, Kaszaki J (2013) Inflammatory activation after experimental cardiac tamponade. *Eur Surg Res.* **51(1-2):**1-13. **IF: 0,75**

II.   Érces D*, **Nógrády M***, Varga G, Szűcs S, Mészáros AT, Fischer-Szatmári T, Cao C, Okada N, Okada H, Boros M, Kaszaki J (2016) Complement C5a inhibition improves late hemodynamic and inflammatory changes in a rat model of nonocclusive mesenteric ischemia. *Surgery* **159(3):**960-71. **IF: 3,38**

III.   Érces D, **Nógrády M**, Nagy E, Varga G, Vass A, Süveges G, Imai M, Okada N, Okada H, Boros M, Kaszaki J (2013) Complement C5A antagonist treatment improves the acute circulatory and inflammatory consequences of experimental cardiac tamponade. *Crit Care Med.* **41(11):**e344-51. **IF: 6,12**

IV.   **Nógrády M**, Varga G, Szűcs Sz, Kaszaki J, Boros M, Érces D (2016) Komplement C5a antagonista terápia hatása nem okkluzív mezenteriális iszkémia állatmodelljeiben *Magyar Sebészet* (accepted)

* the two authors contributed equally

CONTENTS

LIST OF ABBREVIATIONS

AcPepA	acetyl-peptide-A
AMI	acute mesenteric ischemia
big-ET	big-endothelin
CLSEM	confocal laser scanning endomicroscopy
CO	cardiac output
CVP	central venous pressure
C5L2	C5a-like receptor 2
DSA	digital subtraction angiography
ET	endothelin
ET-1	endothelin-1
GI	gastrointestinal
HMGB-1	high mobility group box 1 protein
HR	heart rate
im	intramuscular
ip	intraperitoneal
I/R	ischemia/reperfusion
iv	intravenous
MAP	mean arterial pressure
MAPC	mean arterial pressure of the carotid artery
MAPF	mean arterial pressure of the femoral artery
MPO	myeloperoxidase
NO	nitric oxide
NOMI	nonocclusive mesenteric ischemia
PAO	partial aorta occlusion
PGE_1	Prostaglandin E_1 ,alprostadil
PGE_2	Prostaglandin E_2 ,epoprostenol
PT	pericardial tamponade
RBCV	red blood cell velocity
ROS	reactive oxygen species
SMA	superior mesenteric artery
TNF-α	tumor necrosis factor-α

SUMMARY

Nonocclusive mesenteric ischemia (NOMI) can develop in the absence of apparent anatomical obstruction of the mesenteric circulation in a variety of low flow states. The pathophysiology of NOMI is unexplored, the early diagnosis is challenging and the available treatments are of questionable effectiveness. In this respect, new experimental models are sought to clarify the exact pathomechanisms and new, effective therapeutic ways are needed to reduce the increasingly high mortality. Our first aim was to develop clinically relevant *in vivo* models to investigate the macro- and microcirculatory effects of NOMI. Also, we hypothesized the role of complement activation in the acute and subacute consequences of NOMI and our objectives were to characterize the effects of the inhibition of complement protein known as C5a during this condition. Acetyl-peptide-A (AcPepA) is an antisense-homology box-derived peptide, which is capable to inhibit the C5a effects by binding directly to the anaphylatoxin. We hypothesized that the inhibition of C5a can decrease the intensity of inflammatory reactions and in parallel, to normalize the impaired mesenteric circulation.

Acute experimental pericardial tamponade (PT) was established in anesthetized minipigs, while partial aorta occlusion (PAO) was induced in rats to investigate the circulatory and inflammatory changes of NOMI in clinically relevant time frames. After the relief of PT, elevated levels of oxidative stress markers and inflammatory mediators were detected in association with the signs of diminished splanchnic microcirculation. 24 hours after PAO the macrocirculatory parameters improved significantly, while the intramural microcirculation was significantly impaired and accompanied by increased leukocyte infiltration. The *in vivo* histology confirmed the structural and microvascular damage of the mucosa.

In both animal models of NOMI, the administration of AcPepA moderated the hemodynamic changes, improved the intramural microcirculation, reduced the inflammatory activations and the histological signs of mucosal damage. In conclusion we can say that our newly developed animal models provide a cross section for events in the short and long time frames and proved to be suitable for the investigations of the pathophysiology of NOMI. The hemodynamic changes in the acute PT together with those observed after PAO suggest that complement activation plays central role in the early and late macro- and microcirculatory disturbances during NOMI. The results suggest that C5a inhibitor treatment influences favourably the hemodynamic effects and reduces the potentially harmful inflammatory activation after experimental NOMI as well.

1. INTRODUCTION

1.1. Acute mesenteric ischemia

Acute mesenteric ischemia (AMI) is a serious, life-threatening condition with an approximately 50-70% mortality rate and considered as a vascular emergency with urgency that is comparable to myocardial infarction or apoplexy (1). Arrhythmia, ischemic heart disease, atherosclerosis, endocarditis and cardiomyopathies are among the most important risk factors for AMI (2). Transient decreases of the mesenteric blood flow may cause minimal mucosal lesions only, but if prolonged, splanchnic ischemia leads inevitably to transmural bowel necrosis and perforation (3). Besides, it is also recognized that inadequate intestinal blood supply can lead to secondary inflammatory activation, which reduces the integrity of the bowel wall in the long run (4).

AMI is most often classified as occlusive or non-occlusive. The main causes of occlusive AMI are embolus or thrombus of the superior mesenteric artery (SMA) and mesenteric venous thrombosis (see details in Table 1). Non-occlusive mesenteric ischemia (NOMI), however, evolves in the absence of apparent anatomical obstruction of the mesenteric circulation in a variety of low flow states. Although it may account for 20-30% of AMI cases and different degrees of NOMI occur in many patients with unstable systemic circulatory conditions, including hemorrhagic shock (5), burn injury (6), pancreatitis (7) and the postoperative phase of cardiac and aortic surgery (8), it often remains undiagnosed (9).

The mortality rate of NOMI is constantly high (approximately 50-70%), which highlights the need for prompt diagnosis and adequate treatment (10). Treatment is more likely to be effective, if started early after the onset of signs and symptoms, because the mortality increases exponentially after 6-8 hours (11). While the success rate of surgical treatments of occlusive AMI improved during the last decades, this has remained poor for NOMI (12).

Clinical manifestation, risk factors and classification of AMI

AMI

Arterial occlusive	Arterial nonocclusive	Venous
Embolus or thrombus caused sudden occlusion of the SMA	Reactive vessel spasm in the mesenteric area and decreased CO caused ischemia	Thrombosis in the mesentericportal venous system

Predisposition

Cardiac arrythmia, atrial fibrillation, coronary heart disease, clinical status following myocardial infarction, peripheral occlusive disease	Clinical status following heart surgery with extracorporeal circulation, long-term hemodialysis, digitalis medication	Paraneoplasia, pancreatitis, pancreatic carcinoma, congenital thrombophilia, hepatocellular carcinoma with macrovascular invasion

Clinical manifestations

Abdominal pain, pain-free interval approximately 6 to 12 hrs after symtom onset, subsequent gangrene of the intestine with peritonitis	Increasing abdominal pain or if the patients are not responsive, abdominal distension increase in inflammatory parameters, signs of sepsis	Dependent on severity of thrombosis, often nonspecific abdominal complaints, venous infarction with peritonitis in a minority of cases

Table 1. Clinical manifestation, risk factors and classification of acute mesenteric ischemia (cited from Karl E et. al 2012)

1.2. The pathomechanism of NOMI

Almost any condition that can induce circulatory shock may precipitate NOMI. Circulatory shock is defined as a state of cellular and tissue hypoxia due to reduced oxygen transport and/or increased oxygen consumption or inadequate oxygen utilization. The shock can be divided into four main groups: cardiogenic, distributive, hypovolemic and obstructive. In cardiogenic shock, the intravascular volume is proper, but there is a decreased cardiac output (CO) caused by the failure of the heart to pump effectively. In distributive shock, the peripheral vascular resistance is reduced to a large extent, while hypovolemic shock is caused by the reduction of circulating blood volume. Obstructive shock is due to obstruction of the heart or major blood vessels.

Information on the pathogenesis of NOMI is rather scarce, but it is assumed that the potentially life-threatening structural damage of the mucosa is associated with excessive and sustained splanchnic vasoconstriction (9). NOMI is frequently seen in obstructive shock states when an extramesenteric mechanical obstruction can be found in the underlying pathology. The major causes are tension pneumothorax, constrictive pericarditis or pericardial tamponade as a result of effusion of blood, pus, fluid, or gas into the pericardial sac (13).

Indeed, it has been shown that cardiac tamponade is accompanied by the release of different types of vasopressors (14) with a concomitant elevation of peripheral vascular resistance. The increased afterload may subsequently worsen the hypoperfusion of peripheral organs and results in an increased oxygen demand of the myocardium. The generalized hemodynamic impairment is characterized by a circulatory redistribution leading to regional hypoperfusion of the splanchnic area with NOMI and gastrointestinal (GI) mucosal damage (15, 16).

The deficit in the delivery of intestinal blood provokes mesenteric vasoconstriction (17). Splanchnic hypoxia causes the activation of several endogenous vasoconstrictor mechanisms including the endothelin-1 (ET-1) system (18). ET-1 may compromise the intestinal mucosal circulation by increasing capillary permeability and reducing lymphatic flow leading to interstitial edema (19). Histamine is generally released in various types of tissue ischemia and increases the permeability of the capillaries. ET-1 can also cause histamine release by the degranulation of mast cells (20). High-mobility group box protein-1 (HMGB-1), released passively by necrotic and damaged cells, has been recently identified as

an important signal for leukocyte recruitment (21). The microcirculatory dysfunction in NOMI seems to be mediated by the imbalance of vasoconstrictor and vasodilator molecules, such as ET-1 and nitric oxide (NO). This may also lead to increased leukocyte-endothelial cell interactions, no-reflow phenomenon with plugging of neutrophils, release of proinflammatory cytokines, oxidative stress and ultimately to hypoxic cell injury (22). Moreover, the activation of the complement cascade was described as well (23).

Importantly, the reoxygenation can generate a more severe tissue injury than ischemia alone (24). During the reperfusion phase, the mesenteric blood flow decreases, the mesenteric vascular resistance increases, and the accumulation and free radical production capacity of the leukocytes rises (25). The elevated level of reactive oxygen species (ROS) plays a central role in this phase of the ischemia/reperfusion (IR) process (26, 27). Other endogenous compounds such as platelet-activating factor (28), ET-1 (25), histamine (29), TNF-α (30) and interleukins (31) play also an important role in the final tissue damage. More importantly, the IR can activate the immune system, including the complement system, via antigen-independent inflammatory pathways (32).

1.3. The role of the complement system in NOMI-caused hypoxia and inflammation

An increasing amount of indirect data suggests a central role for the innate immune system in the pathomechanism of NOMI. The complement system is made up of a number of distinct plasma proteins that react with each another in order to opsonize pathogens and induce a series of inflammatory responses that help to fight against infection.

A number of complement proteins belong to the group of proteases that are themselves activated by proteolytic cleavage (33). Complement activation is known to occur through three different pathways: the classical, the alternative and the lectin pathways, involving proteins that mostly exist as inactive zymogens that are then sequentially cleaved and activated (Figure 1). All these pathways converge at C3 (which is the most abundant complement protein found in the blood), provoking the formation of the activation products, C3a, C3b, C5a and the membrane attack complex (C5b-9) (34).

As a consequence of hypoxia and reoxygenation, significant amounts of anaphylatoxin C5a may be produced (35). The C5a fragment, a biologically active side-product of the complement cascade can induce smooth muscle contraction, chemotaxis, and the activation of

neutrophils (36) with the release of ROS and cytokines (37–40). C5a receptors are expressed not only on inflammatory leukocytes, but also on other cell types such as epithelial, endothelial, smooth muscle and other parenchymal cells of solid organs including liver, kidney, and lung. Furthermore, those C5aRs are extremely upregulated at an acute inflammatory state (41).

Complement activation is further enhanced by the bacterial translocation through the hypoperfused intestinal mucosa (42), a process accompanied by the excessive release of ET-1 (23, 43), which might contribute to a further impairment of the microcirculation due to its vasoconstrictor and pro-adhesive effects (44). Furthermore, the release of HMGB-1 is also directly mediated by C5a through C5a-like receptor 2 binding (C5L2) (45). HMGB-1 is an important factor of leukocyte recruitment, inducing the release of other proinflammatory cytokines (46).
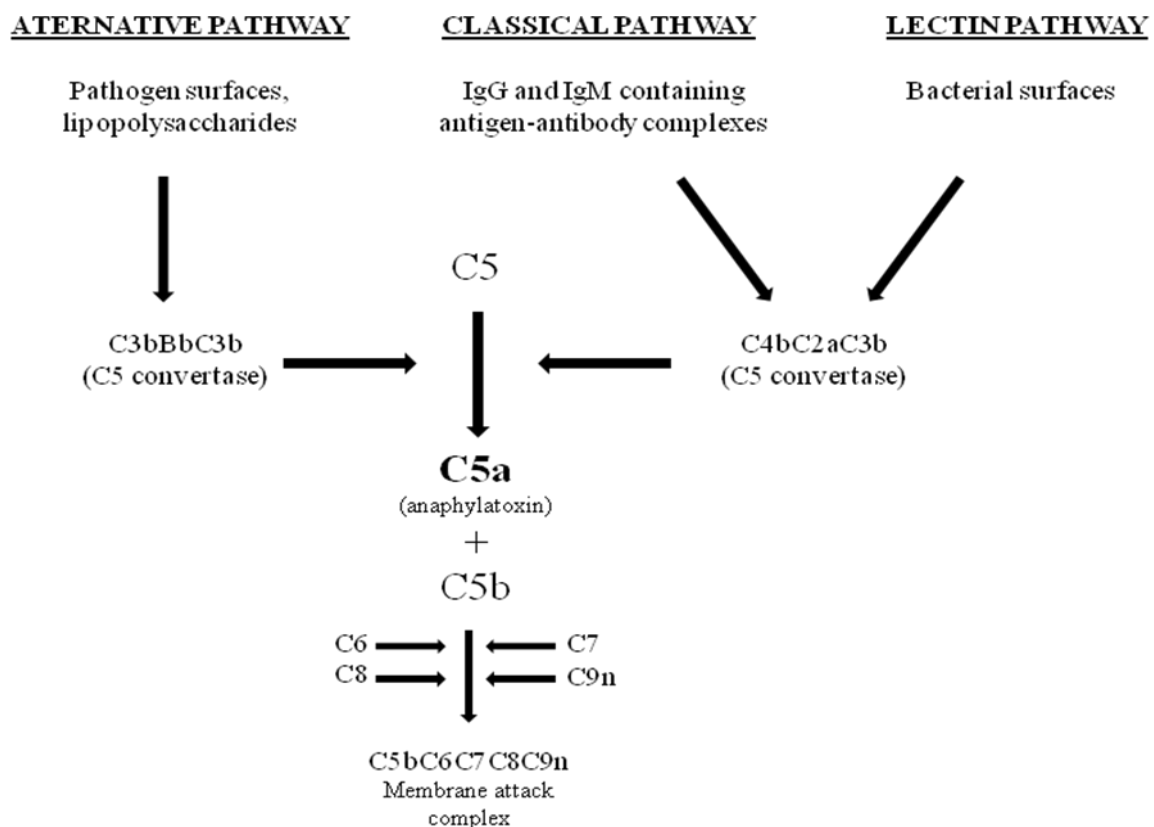

Figure 1. Schematic illustration of the activation of the C5a complement factor in the complement system (after Sarma JV et al. 2011).

1.4. Possibilities of C5a inhibition, the acetyl-peptide-A

Today, there are two main ways to have influence on C5a effects. One of the possibilities is the inhibition by means of anti-C5a antibodies and soluble receptors. However, these larger molecules are unstable, their production is expensive and biological side effects are also expected (47). The other alternative is the use of C5a receptor antagonists. Nevertheless, the usage of these antagonists has also lead to unintended consequences, mainly due to C5a receptor polymorphism (48).

A relatively new solution is the administration of acetyl-peptide-A (AcPepA). The acetylated N-terminal alanine (synthesized and purified (>95% purity) by Biologica, Nagoya, Japan) containing PepA (ASGAPAPGPAGPLRPMF) is an antisense homology box-derived peptide, which is capable of binding directly to C5a in its 37–53 amino acid region. It is important to note that the binding between the peptide and the C5a is not an antigen-antibody interaction.

It has been shown that this anti-C5a peptide is more effective than C5a receptor inhibitors. AcPepA has proved to be highly effective in endotoxin shock pilot studies (49, 50). More importantly, the administration of AcPepA elevated the mean arterial pressure (MAP), did not affect the cardiac output, and caused a significant decrease in the heart rate (HR) in a previous study with experimental cardiac tamponade (51).

1.5. Treatment options in NOMI

All patients with suspected AMI should undergo volume resuscitation and treatment with broad-spectrum antibiotics. The correction of any potential underlying mechanisms of AMI such as arrhythmias or congestive heart failure is necessary (52). Similarly to occlusive AMI, the conservative therapy of NOMI is non-specific and usually limited to hemodynamic support and the correction of biochemical alterations (9).

The first step in suspected NOMI is the catheter angiography (DSA, Class I recommendation, level B of evidence, according to The American College of Cardiology /American Heart Association guidelines), and the treatment of choice is the selective application of vasodilators into the SMA (PGE$_1$ alprostadil in 20 μg bolus followed by a perfusor-directed 60-80 μg/24 hours doses; alternative method is PGI$_2$ epoprostenol 5 to 6 ng/kg/min and intravenous (*iv*) heparin 20 000 IU/24 hours). This protocol is intended to

interrupt the generalized vascular spasm. For patients with suspected NOMI who generally require catecholamine therapy, vasodilators are largely catabolized as they pass through the liver, thus no systemic effect or consecutive neutralization of the effect of catecholamine is to be expected. Follow-up angiography is used to verify the efficiency of vasodilation. Surgery is required only when clinical evidence of peritonitis is present, or for intubated patients with secondary disruption to organ function. It is indicated only for the resection of irreversibly damaged portions of the intestines (11).

Non-surgical management is however, always challenging and precarious, and no vasodilator agent or therapy has gained widespread use so far to prevent the intestinal barrier dysfunction and the subsequent development of transmural gangrene.

1.6. Animal models of NOMI

The consequences of experimental NOMI were investigated in several large animal models. In these cases NOMI is most often induced by pericardial tamponade (PT) (53–57). In other studies, mechanical occlusion of the SMA, noradrenalin infusion into the mesenteric circulation (17) or *iv* digoxin (55) were used. In these studies the short-term consequences of NOMI can be followed, nevertheless, the long-term macro- and microcirculatory consequences of NOMI-induced changes are still unknown.

In large animal PT models the tamponade is induced by filling of the pericardial sack with various fluids such as blood, saline or dextran (58–65). Previously, experimental PT models have been developed by our research group as well (14, 51). In these studies, PT is reproducibly leads to a decline in CO and a significant increase in HR. After relief of the tamponade, a significantly lower MAP and long-lasting impairment of the venous return are observed, while the CO and HR return to normal levels. Briefly, the deterioration of macrohemodynamics after PT is fairly well described, but the splanchnic microcirculatory and inflammatory changes and the long time consequences of NOMI are still unexplored (51).

2. MAIN GOALS

- We hypothesized that experimental PT offers an opportunity to study the pathophysiology of NOMI. Our primary aim was to characterize the effects of PT on the intestinal microcirculatory alterations and inflammatory response in a large animal model.

- We hypothesized that the inhibition of complement component C5a generation would suggest a plausible way to influence the potentially detrimental consequences of NOMI. The aim was to investigate the acute effects of complement C5a inhibitor treatment on NOMI-caused microcirculatory and inflammatory complications.

- Our next aim was to develop a reliable rodent model of NOMI of extramesenteric origin and thus to investigate the major components of local and systemic circulatory reactions. We hypothesized that PAO in rodents leads to an established low-flow condition in the splanchnic area, and this would suggest a plausible way to investigate the pathophysiology of NOMI. Using this new model we decided to characterize the macro- and microcirculatory changes and inflammatory response 24 hours after the initial insult.

- Our aim was to investigate the subsequent effects of AcPepA treatment on NOMI-induced macro- and microcirculatory changes and inflammatory response so as to provide relevant information on the effects of C5a inhibitor therapy in a clinically relevant time frame.

3. MATERIAL AND METHODS

3.1. Animals

The experiments were performed according to the National Institutes of Health guidelines and EU directive 2010/63 for the protection of animals used for scientific purposes and the study was approved by the Ethical Committee for the Protection of Animals in Scientific Research at the University of Szeged (number of approval: V/148/2013).

In *Study I* inbred Vietnamese mini pigs of both sexes (n=19, weighing 24±3 kg) were used. The experiments of *Study II* and *Study III* were performed on male Sprague-Dawley rats (n=31, average weight 350 g).

3.2. Experimental protocol in Study I

The surgical interventions were carried out in minipigs during continuous infusion of propofol (50 µL/min/kg *iv*; 6 mg/kg/hr). Anesthesia was induced by a mixture of ketamine (20 mg/kg) and xylazine (2 mg/kg) intramuscularly (*im*). After endotracheal intubation, the animals were mechanically ventilated with the tidal volume set at 9±2 mL/kg, and the respiratory rate was adjusted to maintain the end-tidal pressure of carbon dioxide and partial pressure of carbon dioxide in the range 35 to 45 mmHg. Positive end-expiratory pressure was not applied during the tamponade. The animals were placed in a supine position on a heating pad for maintenance of the body temperature between 36°C and 37°C and received an infusion of Ringer's lactate solution at a rate of 10 mL/kg/hr during the experiments. The right femoral artery and jugular vein were cannulated for the measurement of MAP and CO by thermodilution method (PICCO Catheters; PULSION Medical Systems, Munich, Germany) and for fluid or drug administration, respectively. After a midline abdominal incision, the root of the SMA was dissected free. An ultrasonic flow probe (Transonic Systems, Ithaca, New York, USA) was placed around the exposed SMA to measure the mesenteric blood flow. In all protocols, the animals were monitored continuously, arterial blood gases were checked regularly (Cobas b121; Roche, Vienna, Austria), and a period of 30 minute was allowed for recovery from surgery.

The animals were randomly allocated to one of the three experimental groups. Group 1 (*n* = 6) served as sham-operated control, with the same time frame and sampling as in groups 2 (*n*=7) and 3 (*n*=6), but without the induction of a cardiac tamponade. Left lateral

thoracotomy was performed in all groups, and in the cardiac tamponade groups, a cannula was fixed in the pericardial cavity. PT was induced for 60 minutes by intrapericardial administration of colloid solution, while the MAP was kept between 40 and 45 mmHg. After this period, the fluid was removed from the pericardial sac and the animals were monitored for 180 minutes following tamponade. Group 3 was treated by AcPepA (a single administration of 4 mg/kg in 5 mL saline *iv* into the jugular vein in a 5-min infusion) after the 45th minute of cardiac tamponade (the beginning of tamponade denotes 0 minute). Vehicle (saline) administration was applied in groups 1 and 2 with the same protocol. Peripheral blood samples were taken at baseline, after 75 and 150 minutes, and at the end of the observation period (240 minutes) to detect the levels of HMGB-1, big-endothelin (big-ET), and whole blood superoxide production. Small intestine tissue biopsies were taken at the end of the experiments for measurement of myeloperoxidase (MPO) activity.

3.3. Experimental protocol in Study II

After intraperitoneal (*ip*) sodium pentobarbital anesthesia (50 mg/kg), the rats were placed in a supine position on heating pads. Tracheostomy was performed to facilitate spontaneous breathing, and the right jugular vein was cannulated by PE50 tubing for drug administration and Ringer-lactate infusion (10 mL/kg/hr). The left carotid artery and the left femoral artery were cannulated for MAP and HR measurements. A catheter equipped with thermistor-tip (PTH-01; Experimetria Ltd., Budapest, Hungary) was positioned into the ascending aorta through the right carotid artery for CO measurements, using thermodilution technique (SPEL Advanced Cardiosys 1.4, Experimetria Ltd, Budapest, Hungary). After a midline abdominal incision, the proximal part of the abdominal aorta was dissected free between the diaphragm and the origin of the SMA and a silicone tourniquet catheter was positioned around the vessel. An ultrasonic flow-probe was placed around the SMA (1RS; Transonic Systems Inc., Ithaca, New York, USA) to measure the flow in SMA. In each group, baseline macrohemodynamic parameters (MAP, CO, SMA flow) were recorded after a 30-minute recovery period. Hemodynamic baseline measurements were taken, in 30 minute after the induction of PAO, before the relief of PAO, at 90 and at 120 minutes.

The animals were randomly divided into two groups. Group 1 (n=7) underwent a 1 hour partial occlusion of the abdominal aorta induced by controlled tightening of the

tourniquet. The goal was to keep MAP in the femoral artery continuously between 30 and 40 mmHg. MAP, CO and SMA flow were recorded at baseline, in 30 minute after the induction of PAO, before the relief of PAO, at 90 and at 120 minutes. Differences in MAP between the femoral (MAPF) and the carotid arteries (MAPC), i.e. above and under the site of PAO, were recorded. Group 2 (n=6) served as sham operated control.

3.4. Experimental protocol in Study III

The rats were placed in a supine position on heating pads and the left femoral artery was cannulated for recording of MAP and HR. After a midline abdominal incision, the proximal part of the abdominal aorta was dissected free between the diaphragm and the origin of the SMA and a silicone tourniquet catheter was positioned around the vessel. A Ringer-lactate infusion (10 mL/kg/hr) was administered *ip* throughout the experiments. The baseline variables were determined during a 30-minute control period.

Group 1 (n=8) served as the sham operated control group, while in group 2 (n=8) and group 3 (n=9), PAO was induced for 1 hour by controlled tightening of the tourniquet. The goal was to maintain MAP in the femoral artery continuously between 30 and 40 mmHg. In groups 1 and 2 the vehicle for AcPepA (infusion of 1 mL saline *iv* for 5 minutes) was injected into the tail vein, while in group 3 the injection of AcPepA (4 mg/kg in 1 mL saline *iv*) into the tail vein started 15 minute prior to the end of PAO. The animals were observed for 90 minutes, the beginning of PAO denotes 0 min. MAP and HR were recorded 4 times (at baseline, at 30 minute after the induction of PAO, before the relief of PAO and 30 minute after the end of PAO). In each group, intravital videomicroscopy was performed in the baseline condition to examine the microcirculation of the serosa of the ileum 5 cm proximally from the cecum (see later). After the observation period, the femoral catheter was carefully removed, the wounds were closed and the animals recovered. In case of any signs of hind limb ischemia, the experiments were terminated and the animals were excluded from the study (n=3).

24 hours after surgery the animals were re-anesthetized (50 mg/kg *ip* sodium pentobarbital), tracheostomy was performed to facilitate spontaneous breathing, and the right jugular vein was cannulated with PE50 tubing for drug administration and Ringer-lactate infusion (10 mL/kg/hr *iv*). The left common carotid artery was cannulated by PE50 tubing for

MAP and HR measurements. A thermistor-tip catheter (PTH-01; Experimetria Ltd., Budapest, Hungary) was positioned into the ascending aorta through the right common carotid artery for CO measurements, using a thermodilution technique with a computer program (SPEL Advanced Cardiosys 1.4, Experimetria Ltd, Budapest, Hungary). The abdominal wound was reopened and an ultrasonic flow-probe was placed around the exposed SMA (1RS; Transonic Systems Inc., Ithaca, New York, USA) to measure the flow of the mesenteric artery. In each group, macrohemodynamic parameters were recorded after a 30-minute recovery period and intravital videomicroscopy was performed to examine the microcirculation of the ileal mucosa 5cm proximally from the cecum. Through another incision, fluorescence confocal laser scanning endomicroscopy (CLSEM) was used for *in vivo* histological investigation. At the end of the experiments, blood samples were taken from the inferior caval vein for determination of plasma TNF-α, HMGB-1 and ET-1 levels. Tissue samples were taken from the ileum for conventional histological examinations and detection of leukocyte accumulation, and then the animals were sacrificed by an overdose of pentobarbital.

3.5. Measurements

3.5.1. Hemodynamic measurements

In *Study I*, central venous pressure (CVP) and blood flow signals were monitored continuously and registered with a computerized data acquisition system (SPELL Haemosys; Experimetria, Budapest, Hungary). The MAP, CO, and HR were measured with the PICCO Plus monitoring system (PULSION Medical Systems; Munich, Germany).

In *Study II and III*, pressure signals (BPR-02 transducer; Experimetria Ltd, Budapest, Hungary) and SMA flow signals (T206 Animal Research Flowmeter; Transonic Systems Inc., Ithaca, New York, USA) were measured continuously and registered also with a computerized data-acquisition system.

3.5.2. Intravital videomicroscopy of the microcirculation

An intravital orthogonal polarization spectral imaging technique (Cytoscan A/R; Cytometrics, Philadelphia, PA) was used for non-invasive visualization of the mucosal microcirculation of the small intestine. This technique utilizes reflected polarized light at the

wavelength of the isosbestic point of oxy- and deoxyhemoglobin (548 nm). As polarization is preserved in reflection, only photons scattered from a depth of 200 to 300 μm contribute to image formation. A ×10 objective was placed onto the serosal surface of the ascending colon, and microscopic images were recorded by a S-VHS video recorder 1 (Panasonic AG-TL 700; Matsushita Electric Ind, Osaka, Japan). Quantitative assessment of the microcirculatory parameters was accomplished off-line by frame-to-frame analysis of the videotaped images. Red blood cell velocity (RBCV, μm/s) changes in the postcapillary venules were determined in three separate fields by means of a computer-assisted image analysis system (IVM Pictron, Budapest, Hungary). All microcirculatory evaluations were performed by the same investigators (MN and GV).

3.5.3. Plasma HMGB-1, big-ET-1, ET-1, TNF-α and histamine measurements

In *Study I*, four ml blood samples were drawn from the jugular vein into chilled polypropylene tubes containing EDTA (1 mg/mL) at baseline, after 75 and 150 min, and at the end of the observation period (240 min). The blood samples were centrifuged at 1,200 g for 10 min at 4 °C. The plasma samples were afterwards collected and stored at -70°C until assay. The plasma concentration of HMGB-1 was measured with a commercially available HMGB-1 ELISA kit (Shino-Test, Kanagawa, Japan). Plasma levels of big-ET, a 38-amino acid precursor protein of ET-1, were measured with a commercially available kit (Biochemica Hungaria Kft., Budapest, Hungary). Plasma histamine concentrations were determined with a commercially available enzyme-linked immunoassay (Quantikine ultrasensitive EIA kit for histamine; Biomedica Hungaria Kft, Budapest, Hungary).

In *Study II and III*, blood samples (0.5 mL) were taken from the inferior caval vein into precooled, heparizined (100 U/mL) polypropylene tubes, and centrifuged at 1,000 g at 4 °C for 30 min and then stored at -70 °C until assay. Plasma TNF-α concentration was determined in duplicate by means of a commercially available enzyme-linked immunosorbent assay (Quantikine ultrasensitive ELISA kit for rat TNF-α; Biomedica Hungaria Kft, Budapest, Hungary). The plasma level of HMGB-1 was measured with a commercially available HMGB-1 ELISA kit. Concentrations of ET-1 in the plasma were examined with a commercially available kit (Biochemica Hungaria Kft., Budapest, Hungary).

3.5.4. MPO activity

The activity of MPO, a marker of neutrophil activation, was determined in ileal biopsy samples according to the method of Kuebler et al (66). Briefly, a reaction mixture containing 50-mM K_3PO_4 buffer (pH 6.0), 2 mM 3,3′,5,5′-tetramethylbenzidine (dissolved in DMSO) and 100 µL of undiluted plasma sample was incubated for 5 min at 37°C. The reaction was started with 0.6 mM hydrogen peroxide (dissolved in 0.75 mL K_3PO_4 buffer) and was stopped after 5 min with 0.2 mL of H_2SO_4 (2 M), and the hydrogen peroxide–dependent oxidation of tetramethylbenzidine was detected by a spectrophotometer at 450 nm (UV-1601 Spectrophotometer; Shimadzu, Kyoto, Japan). MPO levels were calculated via a calibration curve prepared with a MPO standard (Sigma-Aldrich GmbH, Munich, Germany). To detect the tissue MPO activity, ileal samples were homogenized with Tris-HCl buffer (0.1 M, pH 7.4) containing 0.1 mM phenylmethylsulfonyl fluoride to block tissue proteases and then centrifuged at 4°C for 20 min at 24,000 g. The MPO activities of the samples were measured as described above, and the data were referred to the protein content.

3.5.5. Whole blood superoxide production

For the whole blood superoxide production measurements, the chemiluminometric method of Zimmermann et al. (67) was used. During the measurements, 10 µL of whole blood was added to 1-mL Hank's solution (PAA Cell Culture, Westborough, MA) and the mixture was kept at 37°C until assay. The chemiluminometric response was measured with a Lumat LB9507 luminometer (Berthold, Wildbad, Germany) during a 30-min period after the addition of 100 µL of lucigenin.

3.5.6. Histological investigation of leukocyte infiltration in tissues

Full-thickness ileal biopsies taken at the end of the experiments were analysed in each group. The tissue was fixed in 6% buffered formalin, embedded in paraffin, cut into 4-µm-thick sections and stained with hematoxylin and eosin. The infiltration of leukocytes was detected and the number of leukocytes was counted in at least 20 fields of view at an original magnification of 400x.

3.5.7. In vivo detection of structural and microvascular damage of the mucosa –
fluorescence CLSEM

The extent of microvascular damage of the terminal ileum was evaluated by fluorescence CLSEM (Five1; Optiscan Pty. Ltd., Melbourne, Victoria, Australia) developed for *in vivo* histology. Records were taken on day 2 for the observation of the effects of C5a inhibitor treatment. The mucosal surface of the terminal ileum (5 cm proximal to the cecum) was surgically exposed and laid flat for examination.

The microvascular structure was recorded after the *iv* administration of 0.3 ml of fluorescein isothiocyanate-dextran (FITC-dextran 150 kDa, 20 mg/ml solution dissolved in saline, Sigma-Aldrich Inc, St. Louis, MO, USA). The objective lens of the device was placed onto the mucosal surface of the ileum, and confocal imaging was performed 5 min after dye administration (1 scan/image, 1024 x 1024 pixels and 475 x 475 μm per image).

The injury of mucosal architecture was examined following topical application of the fluorescent dye acriflavin (Sigma-Aldrich Inc, St. Louis, MO, USA). The surplus dye was washed off the mucosal surface of the ileum with saline 2 min before imaging. Non-overlapping fields of active areas of PAO were compared to the samples of AcPepA-treated or control groups by using a semiquantitative scoring system with the following criteria: I. the structure of the microvessels (0 = normal, 1 = dye extravasation, but the vessel structure is recognizable, 2 = destruction, and the vessel structure is unrecognizable); II. denudation of villi (0 = no denudation, 1 = at least one area per field of view, 2 = more than one area without a recognizable villi structure per field of view; III. edema (0 = no edema, 1 = moderate epithelial swelling, 2 = severe edema); IV. shedding cells (0 = normal, clearly, well-defined villi structure without shedding cells , 1 = some shedding cells; less than 30 cells per field of view, 2 = shedding cells, more than 30 cells per field of view, 3 = severe debris); V. epithelial gap (0 = no gap, 1 = number of gaps, less than 5 per villi, 2 = number of gaps, more than 5 per villi); VI. longitudinal fissure on villi (0 = no fissure, 1 = presence of fissure). The analysis was performed twice, separately, by two investigators (MN and GV).

3.5.8. Statistical analysis

Data analysis was performed with a statistical software package (SigmaStat for Windows; Jandel Scientific, Erkrath, Germany). Friedman test for repeated-measures analysis of variance on ranks was applied within groups. Time-dependent differences from the baseline for each group were assessed by Dunn's method, and differences between groups were analyzed by Kruskal-Wallis one-way analysis of variance on ranks, followed by Dunn's method for pairwise multiple comparison. Differences between groups in the *Study II* were analysed by Mann-Whitney test, followed by Dunn's method for pairwise multiple comparison. In the figures, median values and 25th and 75th percentiles are given; p values of less than 0.05 were considered as significant.

4. RESULTS

4.1. Hemodynamics

4.1.1. Acute changes in hemodynamics in Study I

A significant decrease in SMA flow indicated redistribution of the mesenteric circulation during the tamponade. After the removal of the pericardial fluid, the SMA flow returned to the control values. Administration of AcPepA after 45 min of cardiac tamponade resulted in a significant elevation of the SMA flow in the post-tamponade period (**Figure 2A**).

A heterogeneous, oscillating microcirculation was present in the small intestinal mucosa in all groups, and therefore, the weighted average of RBCV was calculated. This was based on the duration of the fast and slow flow periods and the RBCV during the respective phases, as reported previously (68). The RBCV during the fast flow periods showed no change in the sham-operated group, but at the end of the cardiac tamponade, a significant decrease from the baseline was observed in the group where cardiac tamponade was not used (**Figure 2B**). By the end of the post-tamponade phase, in the AcPepA-treated group, it was significantly increased regarding the baseline level and also relative to the non-treated group (cardiac tamponade group: M = 641.3; p25 = 584.5; p75 = 684.7 μm/s vs AcPepA group: M = 1,031.3; p25 = 935.3; p75 = 1108.3 μm/s). The duration of the slow flow period in the cardiac tamponade group increased significantly at 240 min, but it was reduced in the treated group (cardiac tamponade group: M = 15.01; p25 = 12.56; p75 = 17.56 s vs AcPepA group: M = 7.65; p25 = 7.33; p75 = 8.67 s). By the end of the experiments, the characteristic variable of the mucosal microcirculation, the average RBCV of the flow pattern, was significantly reduced in the cardiac tamponade group if compared to the AcPepA group (**Figure 2B**).
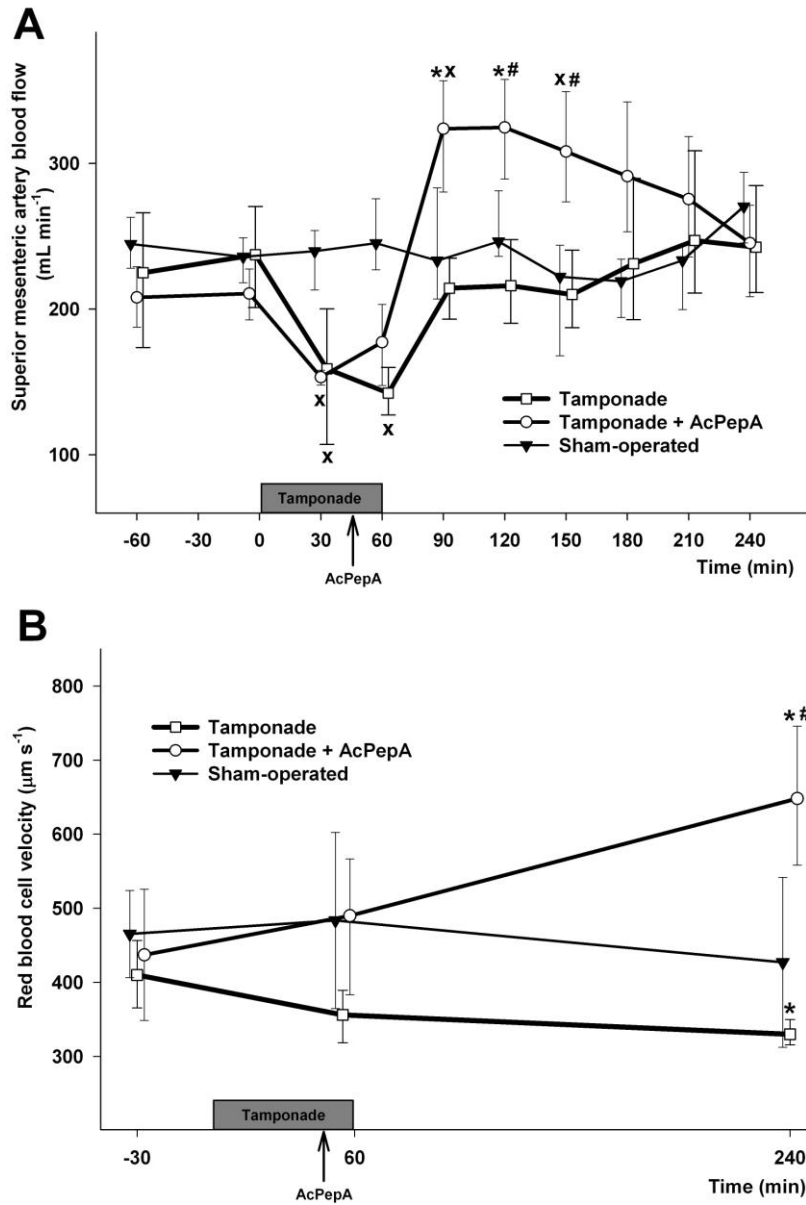
Figure 2. Changes in superior mesenteric artery blood flow (**A**) and average red blood cell velocity (**B**) in the sham-operated ($n = 6$; *solid triangles with continuous line*), cardiac tamponade ($n = 7$; *empty squares with solid line*), and AcPepA-treated ($n = 6$; *empty circles with solid line*) groups. The *box* indicates the duration of the cardiac tamponade; the *arrow* shows the treatment with AcPepA. The plots demonstrate the median values and the 25th (*lower whisker*) and 75th (*upper whisker*) percentiles; * $p < 0.05$ within groups versus baseline values (Friedman repeated-measures analysis of variance on ranks followed by Dunn's method), x $p < 0.05$ between groups versus sham-operated group values (Kruskal-Wallis one-way analysis of variance on ranks, followed by Dunn's method), and # $p < 0.05$ between AcPepA-treated group and cardiac tamponade group (Kruskal-Wallis one-way analysis of variance on ranks, followed by Dunn's method).

4.1.2. Acute hemodynamic changes in Study II

In these experiments MAP, CO and the SMA flow were monitored to gain information about the circulatory changes induced by PAO and to verify the decrease in the SMA flow. During PAO, while the MAPF was kept between 30-40 mmHg, the MAPC was significantly increased initially compared to both the baseline values of the general MAP and to the MAPC values in the sham operated group, however later it was significantly different only from the baseline values. The CO started to decrease after 30 min of PAO and reached a significant difference compared to the sham operated group and to the baseline values by the end of PAO.

MAP was significantly increased in 30 min after the relief of PAO and then returned gradually to the control values by the end of the observation period. The CO started to increase after the PAO and no significant differences could be detected during the post-occlusion period. The SMA flow decreased significantly during the PAO and remained significantly lower compared to the baseline and sham operated values until the end of the experiments (Table 2).

			MAP during PAO on Day 1			
	Parameters	Baseline	30 min (Carotid artery)	60 min (Carotid artery)	90 min	120 min
			30 min (Femoral artery)	60 min (Femoral artery)		
Sham operated	**Median**	**106.0**	**107.0**	**112.5**	**103.5**	**108.2**
	25p; 75p	*88.9; 111.2*	*88.9; 119.7*	*87.63; 122.1*	*86.1; 116.0*	*67.6; 122.5*
			105.5	**109.6**		
			90.5; 113.3	*89.5; 122.0*		
PAO	**Median**	**107.5**	**147.0*x**	**133.1***	**128.5*x**	**109.3**
	25p; 75p	*99.0; 113.8*	*139.8; 158.8*	*121.8; 142.5*	*122.0; 135.2*	*103.4; 119.1*
			37.5*x	**37.5*x**		
			31.8; 41.3	*30.7; 41.2*		

CO during PAO on Day 1

	Parameters	Baseline	30 min	60 min	90 min	120 min
Sham operated	**Median**	**210**	**216**	**217**	**204**	**216**
	25p; 75p	*205; 217*	*197; 229*	*187; 237*	*195; 232*	*189; 225*
PAO	**Median**	**206**	**206**	**164*x**	**184**	**203**
	25p; 75p	*200; 214*	*181; 250*	*150; 178*	*173; 210*	*181; 225*

SMA flow during PAO on Day 1

	Parameters	Baseline	30 min	60 min	90 min	120 min
Sham operated	**Median**	**14.2**	**14.0**	**14.9**	**14.6**	**15.2**
	25p; 75p	*12.3; 16.0*	*11.8; 17.0*	*14.1; 15.8*	*13.6; 19.7*	*12.5; 18.6*
PAO	**Median**	**15.3**	**1.4*x**	**2.1*x**	**10.8*x**	**8.6*x**
	25p; 75p	*13.8; 15.6*	*1.8; 2.1*	*1.2; 2.6*	*9.2; 12.1*	*8.3; 10.2*

Table 2. Changes in MAP [mmHg], CO [mL min^{-1} kg^{-1}] and SMA flow [mL min^{-1}] on Day 1. * $p<0.05$ within groups *vs* baseline values (Friedman and Dunn test); [x] $p<0.05$ PAO group *vs* sham-operated group (Mann-Whitney and Dunn test).

4.1.3. Hemodynamic changes in Study III

In the sham operated animals, there were no significant changes in the MAP on day 1. In the groups with PAO, the MAP was kept between 30-40 mmHg for 60 min. The MAP was significantly higher in the PAO group compared to the control group 30 min after the relief of aorta occlusion. AcPepA treatment did not influence these parameters. No difference was found between the groups in the parameters of serosal microcirculation, when measured in the control period before PAO (**Figure 3A**).

On day 2, the MAP did not differ between the groups or the baseline values of day 1. The surgical interventions caused an increase in HR by day 2. Nonetheless, the HR was significantly higher in the PAO group compared to the sham operated animals, while after AcPepA treatment, the HR did not increase significantly in respect of the values of the sham operated group (**Figure 3B**). The SMA flow in the treated group remained at the control level, while in the non-treated group it was significantly higher in comparison with the sham operated group. The elevated CO was significantly decreased following C5a inhibitor

treatment on day 2 (**Figure 4**). On day 2, both the serosal and mucosal RBCV were significantly decreased in comparison with the sham operated group. AcPepA treatment resulted in a significantly higher RBCV (**Figure 5AB**).
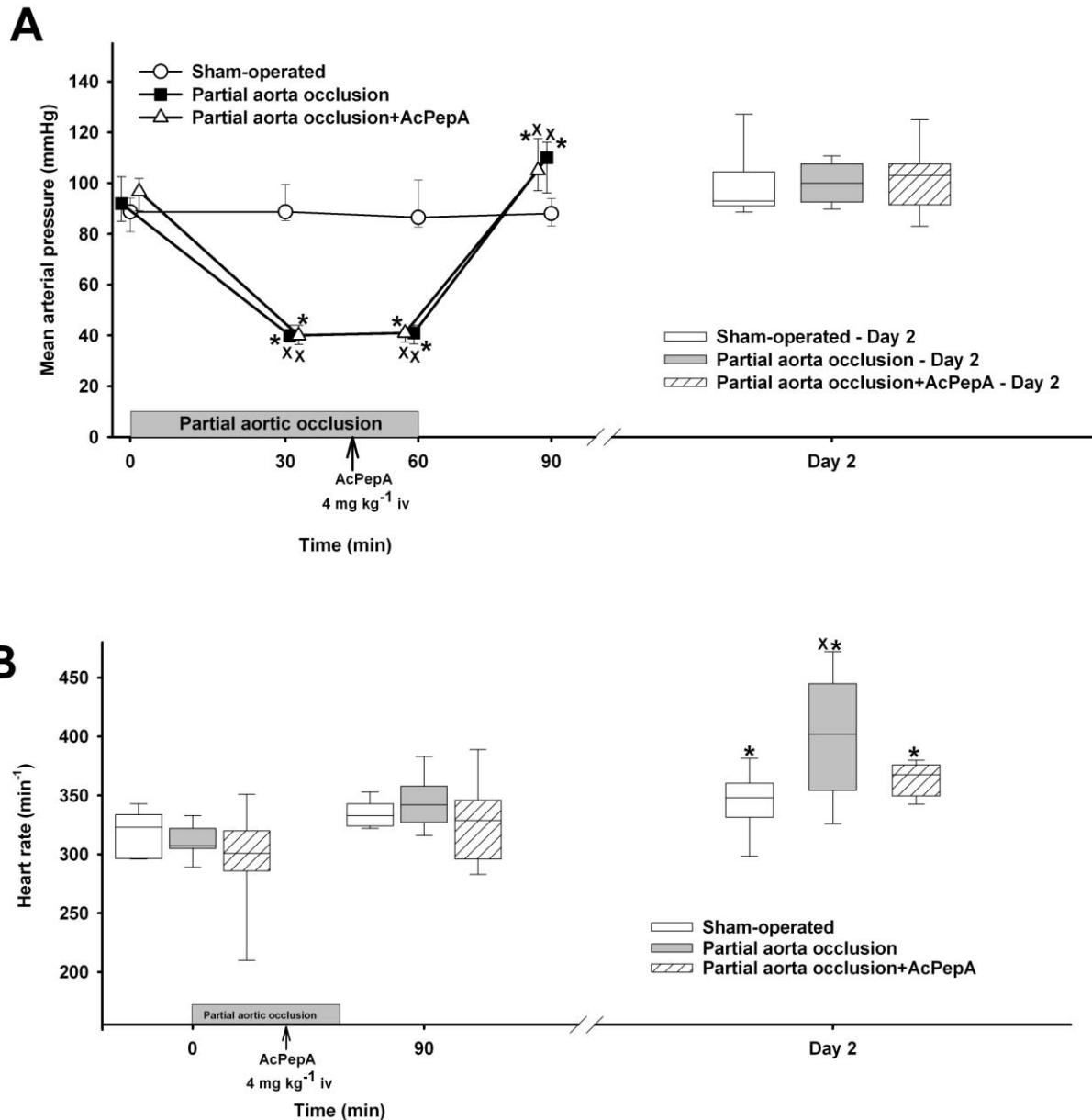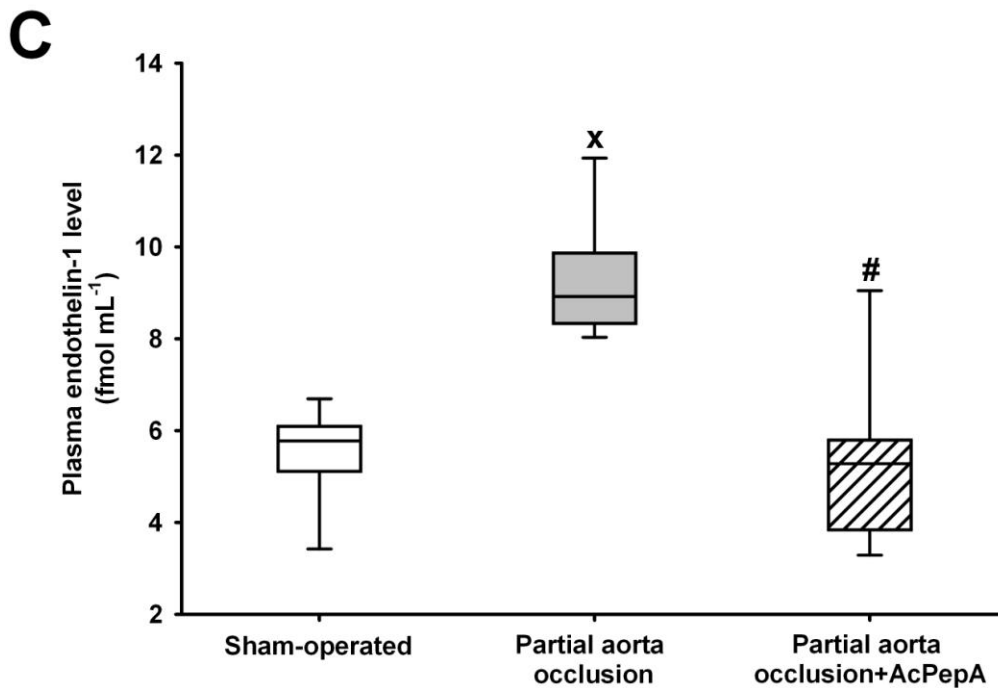

Figure 3. Changes in MAP in the sham operated (empty circles with thin continuous line; empty box), PAO (black squares with continuous line; gray box) and PAO+AcPepA (empty triangles with continuous line; striped empty box) groups (**A**). The plots demonstrate the median (horizontal line in the box) and the 25th and 75th percentiles. * $p < 0.05$ within groups *vs* baseline values, [x] $p < 0.05$ between groups *vs* control group values. Changes in heart rate in the control (empty box), PAO (gray box) and PAO+AcPepA (striped empty box) groups (**B**). The plots demonstrate the median (horizontal line in the box) and the 25th and 75th percentiles. * $p < 0.05$ within groups *vs* baseline values, [x] $p < 0.05$ between groups *vs* control group values.
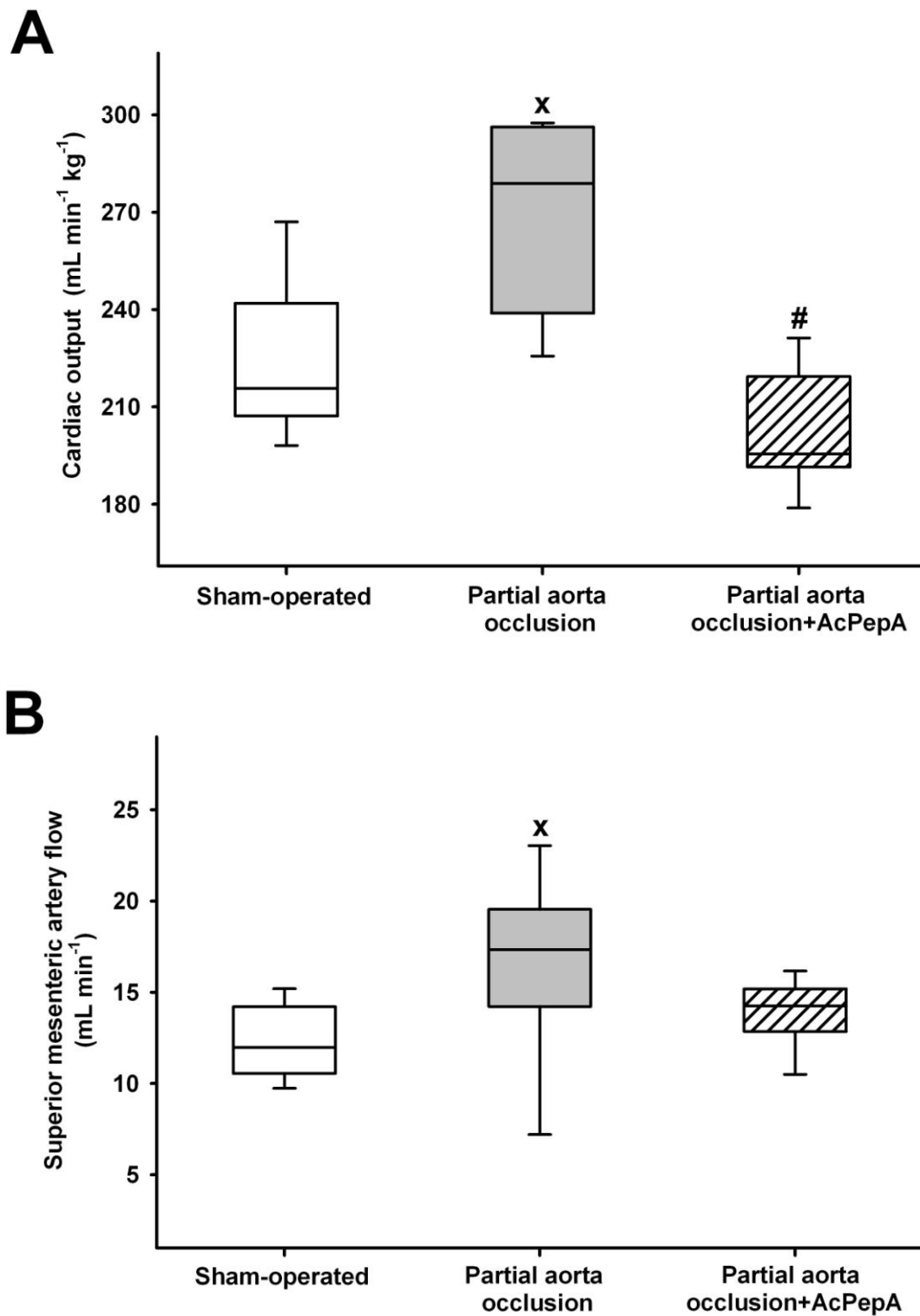
Figure 4. Changes in CO index **(A)** and in SMA flow **(B)** in the sham operated (empty box), PAO (gray box) and PAO+AcPepA (striped empty box) groups. The plots demonstrate the median (horizontal line in the box) and the 25th and 75th percentiles. [x] $p<0.05$ between groups *vs* control group values.
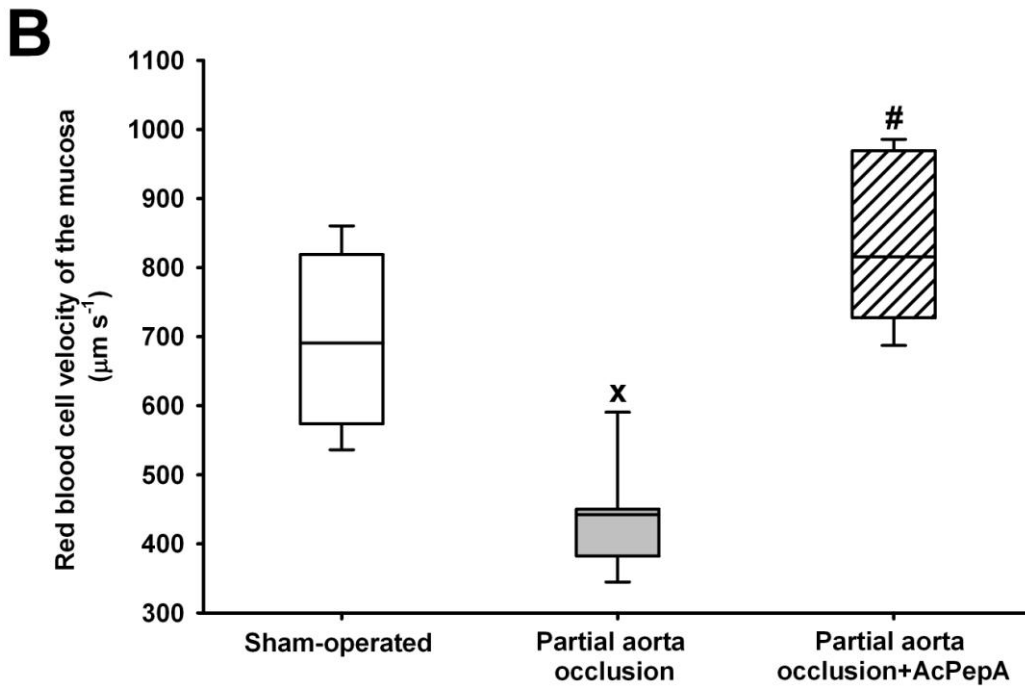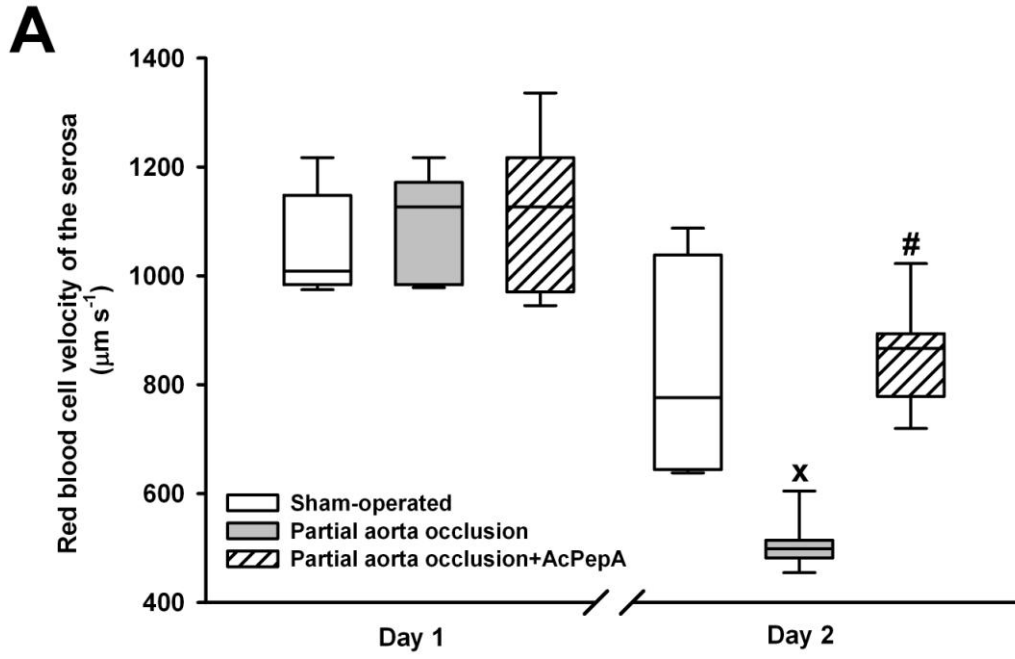
Figure 5. Changes in serosal **(A)**, mucosal **(B)** RBCV and plasma ET-1 levels **(C)** in the sham operated (empty box), PAO (gray box) and PAO+AcPepA (striped empty box) groups. The plots demonstrate the median (horizontal line in the box) and the 25th and 75th percentiles. # $p<0.05$ between AcPepA-treated group *vs* PAO group.

4.1.4. Microvascular and structural damage of the mucosa in Study III, day 2

The microvessels in the villi were visualized by FITC-dextran administration, while the morphology of the mucosa was examined with acriflavin staining. In the PAO group, the CLSEM evaluation demonstrated significant tissue damage in contrast with the sham operated group (**Figure 6**). The vessel structure was disorganized and fluorescent dye leakage could be observed. The acriflavin staining of the surface of the villi revealed the presence of longitudinal fissure and epithelial gaps and showed large amount of debris (**Figure 7 A-C**).

Administration of the C5a inhibitor AcPepA decreased the mucosal damage and significantly influenced both the changes in the microvascular structure and in the epithelial morphology of the small intestine. These changes were still more prominent than in the sham operated group, but the degree of injury was decreased, as shown by the reduced dye leakage compared to the non treated PAO group (**Figure 7 D-F**).

Figure 6. Level of mucosal injury manifested by CLSEM *in vivo* histological records in the sham operated (empty box), PAO (gray box) and PAO+AcPepA (striped empty box) groups. The plots demonstrate the median (horizontal line in the box) and the 25th and 75th percentiles. x $p<0.05$ between groups *vs* control group values; # $p<0.05$ between AcPepA-treated group and PAO group.
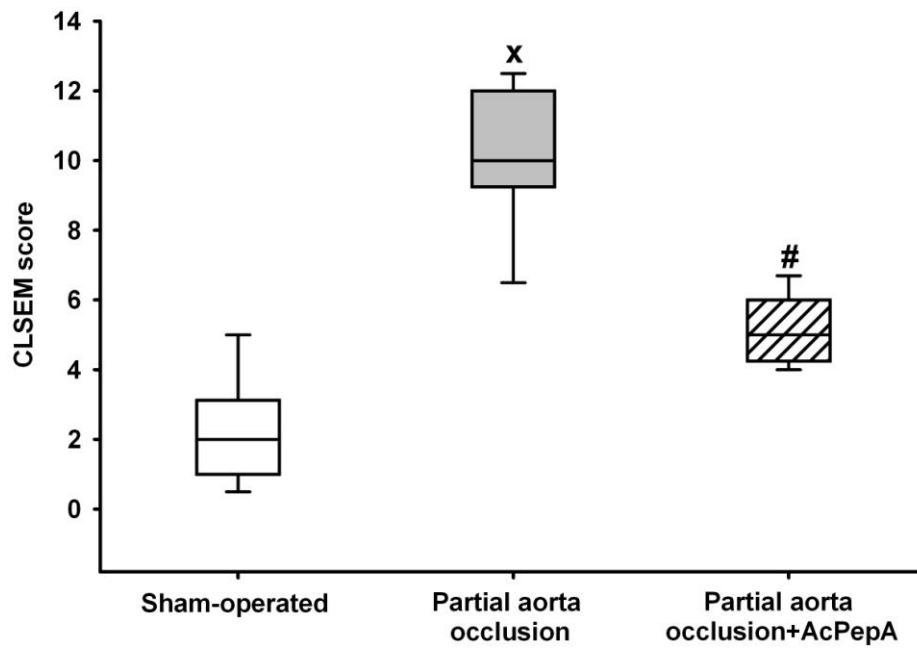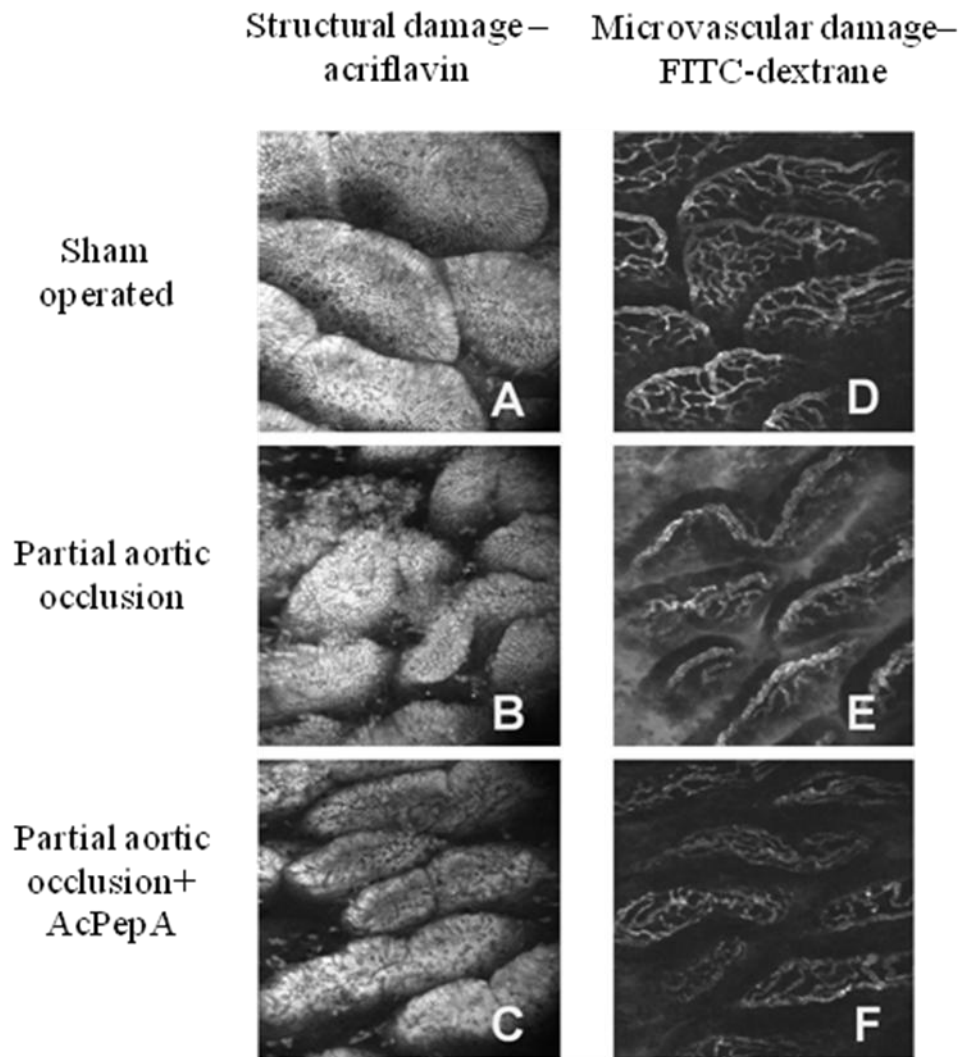
**Figure 7.** *In vivo* histological (CLSEM) records showing the changes of the epithelial surface 24 hrs after the PAO (acriflavin staining) in the sham operated (**A**), PAO (**B**) and PAO+AcPepA (**C**) groups. Alterations in the microvascular structure was visualized with CLSEM after *iv* administration of FITC-dextran in the sham operated (**D**), PAO (**E**) and PAO+AcPepA (**F**) groups.
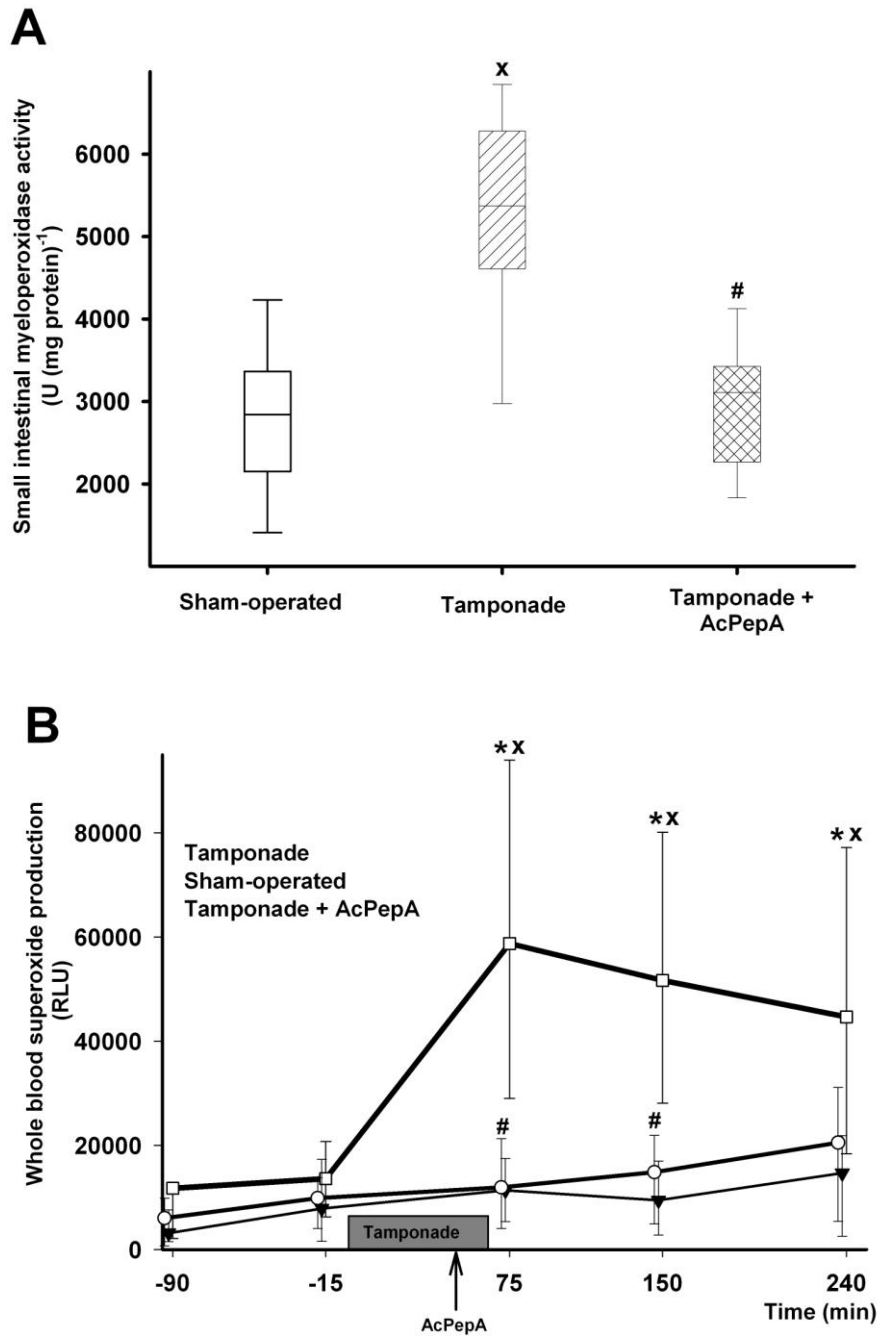
4.2. Biochemical parameters

4.2.1. Changes in biochemical parameters in Study I

Peripheral blood samples were taken at baseline, after 75 and 150 min, and at the end of the observation period (240 min). big-ET is a stable precursor of ET-1 with a longer half-life; it is released from different types of cells. The plasma big-ET levels increased significantly four- to five-fold in the non-treated group after cardiac tamponade (**Figure 8A**). HMGB-1 is a very effective signal for neutrophil activation, which causes an escalation of the inflammatory process. The plasma level of HMGB-1 was elevated significantly after the compression of the heart (**Figure 8B**). The rate of neutrophil accumulation was determined with the help of the measurement of MPO activity of the intestinal tissue samples taken at the end of the experiments. The level of MPO activity was significantly higher in the small intestinal tissue samples of the cardiac tamponade group, indicating the increased accumulation of neutrophils (**Figure 9A**). In the cardiac tamponade group, increased superoxide production was perceptible in the blood at the beginning of the post-tamponade phase (**Figure 9B**). After AcPepA administration, the characteristic biochemical changes following the cardiac tamponade were significantly different. The AcPepA treatment reduced the concentrations of big-ET and HMGB-1 in the plasma. The amount of oxygen free radicals that were formed was also reduced by the treatment, and the MPO activity was decreased as well (**Figures 8-9**).
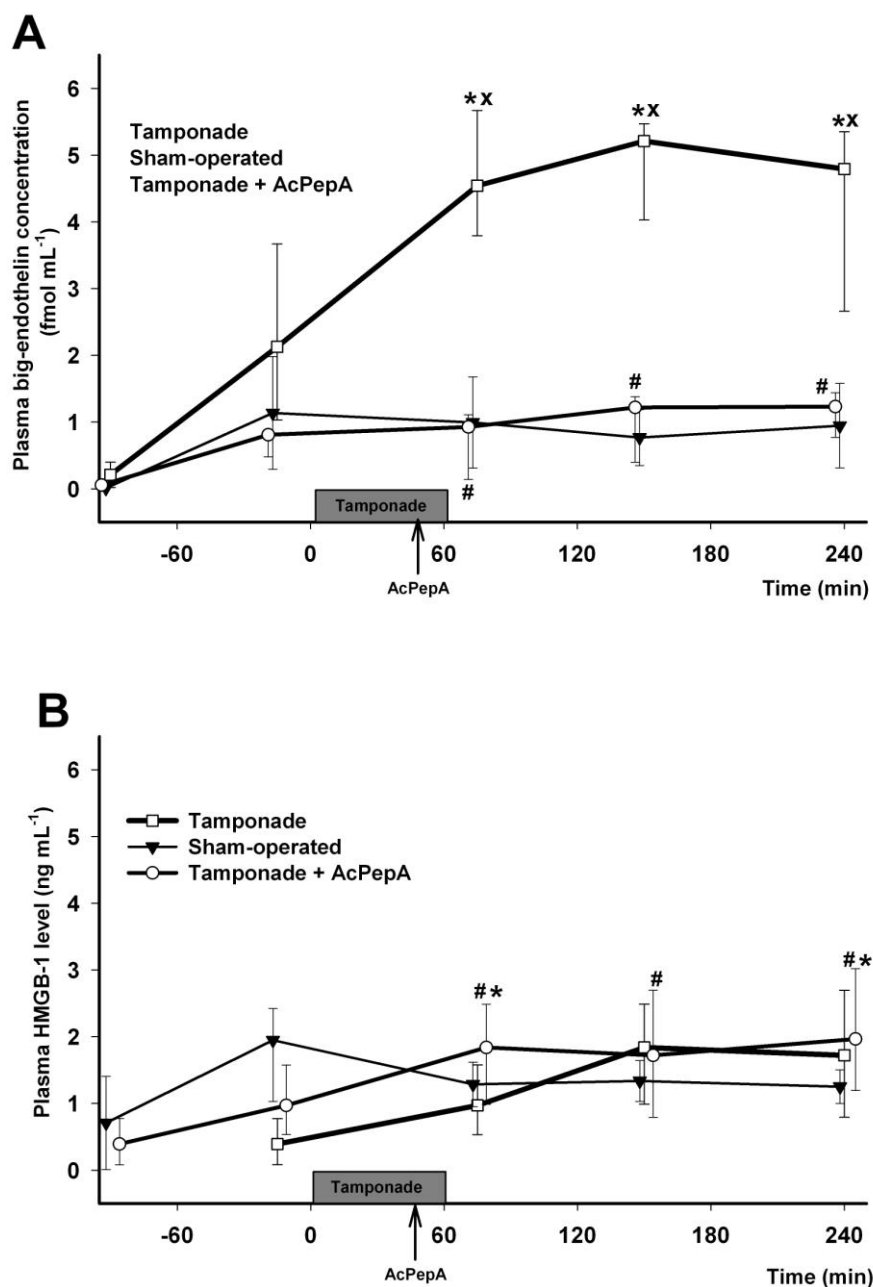
Figure 8. Changes in plasma big-endothelin concentration (**A**), and plasma HMGB-1 level (**B**) in the sham-operated ($n = 6$; *solid triangles with continuous line*), cardiac tamponade ($n = 7$; *empty squares with solid line*), and AcPepA-treated ($n = 6$; *empty circles with solid line*) groups. The *box* indicates the duration of the cardiac tamponade; the *arrow* shows the treatment with AcPepA. The plots demonstrate the median values and the 25th (*lower whisker*) and 75th (*upper whisker*) percentiles; * $p < 0.05$ within groups versus baseline values (Friedman test for repeated-measures analysis of variance on ranks followed by Dunn's method), x $p < 0.05$ between groups *vs* sham-operated group values (Kruskal-Wallis one-way analysis of variance on ranks, followed by Dunn's method), and # $p < 0.05$ between AcPepA-treated group *vs* cardiac tamponade group (Kruskal-Wallis one-way analysis of variance on ranks, followed by Dunn's method).

Figure 9. Changes in small intestinal MPO activity (**A**) in the sham-operated ($n = 6$; *empty box*), cardiac tamponade ($n = 7$; *striped box*), and AcPepA-treated ($n = 6$; *checked box*) groups. Changes in whole blood superoxide production (**B**) in the sham-operated ($n = 6$; *solid triangles with continuous line*), cardiac tamponade ($n = 7$; *empty squares with solid line*) and AcPepA-treated ($n = 6$; *empty circles with solid line*) groups. The *box* indicates the duration of the cardiac tamponade; the *arrow* shows the treatment with AcPepA. The plots demonstrate the median (*horizontal line in the box*) and the 25th and 75th percentiles. * $p < 0.05$ within groups versus baseline values (Friedman test for repeated-measures analysis of variance on ranks followed by Dunn's method), x $p < 0.05$ between groups *vs* sham-operated group values (Kruskal-Wallis one-way analysis of variance on ranks, followed by Dunn's method), and # $p < 0.05$ between AcPepA-treated group *vs* cardiac tamponade group values (Kruskal-Wallis one-way analysis of variance on ranks, followed by Dunn's method).

4.2.2. Changes in biochemical parameters in Study II-III

The concentrations of inflammatory mediators TNF-α and HMGB1 were increased significantly 24 hrs following the ischemic insult. The C5a inhibitor treatment decreased the level of TNF-α, similarly to the concentration of HMGB-1 (**Figure 10AB**). The level of ET-1, an important vasoconstrictor, which can be responsible for the impairment of the mucosal microcirculation, was also elevated on the day after the PAO (**Figure 5C**). The administration of AcPepA was able to decrease the ET-1 concentration significantly.

On the second day of the experiments, significant leukocyte accumulation was observed in the PAO group as compared to the sham operated animals. The administration of AcPepA significantly reduced the leukocyte infiltration of the small intestinal wall (**Figure 10C**).
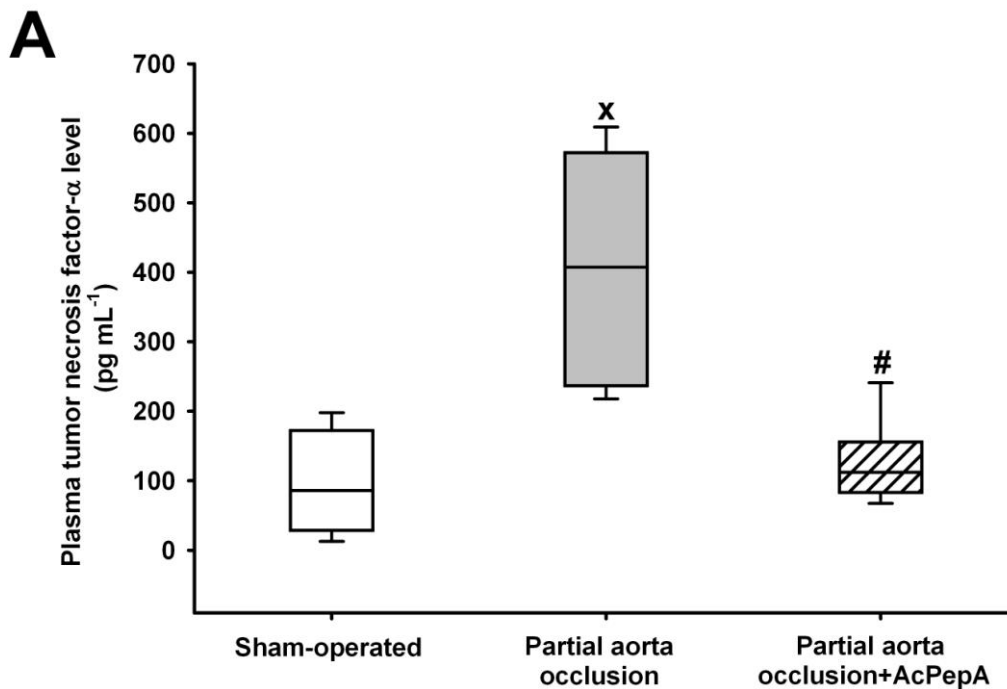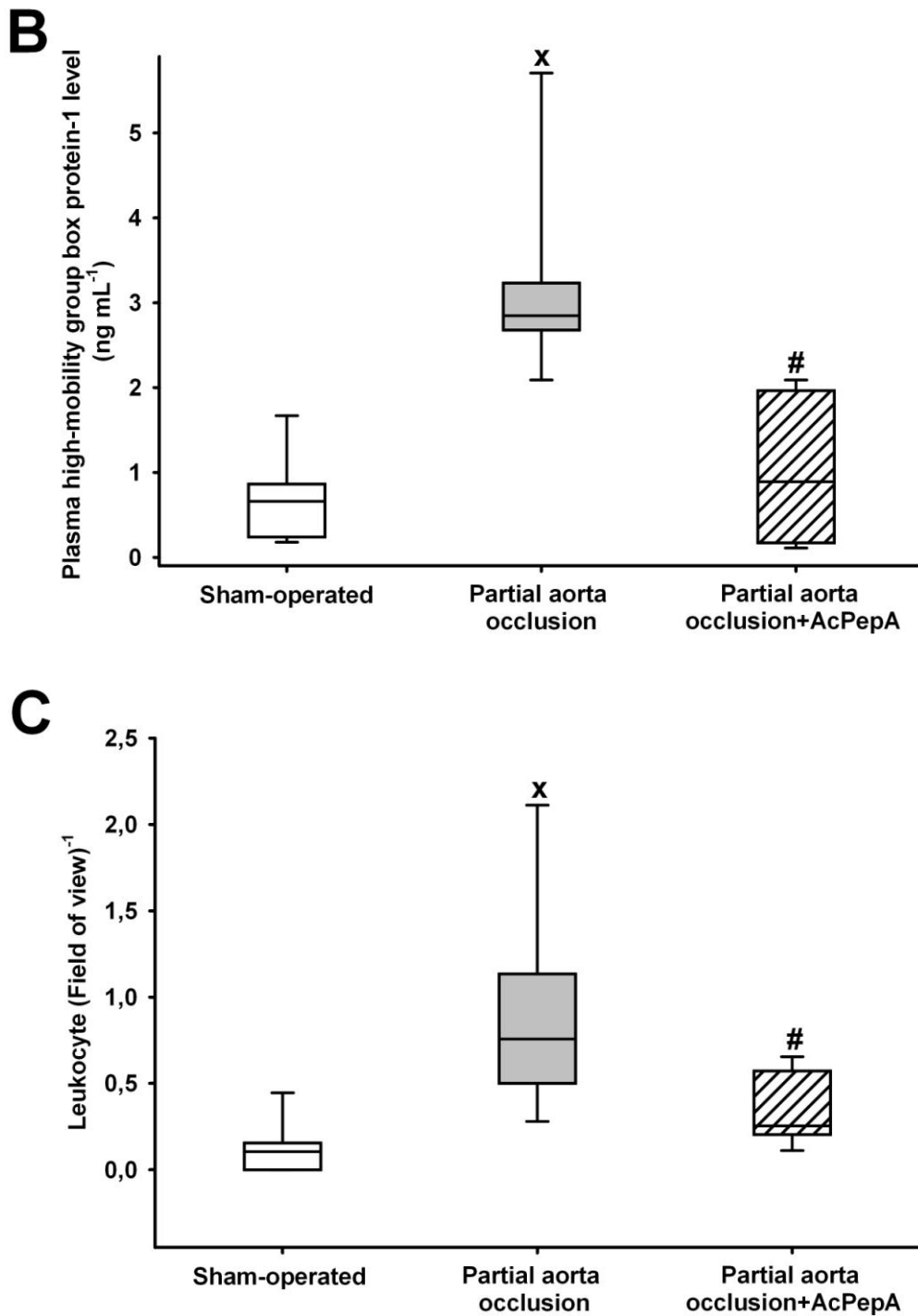
Figure 10. Changes in plasma TNF-α **(A)**, HMGB-1 **(B)** levels and small intestinal leukocyte infiltration **(C)** in the sham operated (empty box), PAO (gray box) and PAO+AcPepA (striped empty box) groups. The plots demonstrate the median (horizontal line in the box) and the 25th and 75th percentiles. [x] $p<0.05$ between groups *vs* control group values; [#] $p<0.05$ between AcPepA-treated group and PAO group.

5. DISCUSSION

5.1. Acute circulatory and inflammatory consequences of experimental cardiac tamponade and complement C5A antagonist treatment: Study I

We have characterized the acute hemodynamic consequences of temporary mechanical compression of the heart. In this setup we have also outlined the consequences of C5a antagonism on the early splanchnic circulatory changes. In this porcine model, the post-tamponade period was characterized by decreased MAP and CVP, whereas the HR was significantly elevated. These acute hemodynamic alterations were accompanied by definite signs of inflammatory activation, with the release of vasoactive and proinflammatory mediators, including histamine, HMGB-1, and big-ET. The deterioration of the systemic circulation was followed by parallel impairment of the microcirculation in the splanchnic area. These changes were accompanied by an increase in local MPO activity, a quantitative marker of ROS-producing neutrophils in the plasma and various tissues (69, 70).

After the relief of the cardiac tamponade, the MAP was decreased, whereas the CO remained compensated, and there were no significant differences if compared to the control group. This was achieved by the elevated HR, which refers to the increased strain of the heart muscle. Following AcPepA treatment, the MAP was elevated compared to the control level and the CO was also maintained. Thus, the most pronounced differences between the compensating mechanisms of treated and non-treated tamponade groups were the restored CO and the lower HR. This seems to be especially crucial if we consider the fact that the circulation of the heart muscle is supplied during the diastolic phase, and it nearly stops during the systole. If the HR is increased, the length of the systole does not change, while the diastole is shortened. A higher frequency results in less time for oxygen delivery to the cardiac muscle cells, and therefore a lower HR and maintained CO provide better oxygenation for the heart. The elevated CVP in the treated group also indicate that the main compensatory mechanism in this early phase is switched from an increased afterload to an elevation of the preload. These changes might be the consequences of reduced ET and histamine release after AcPepA treatment. Indeed, it has been shown that non-selective ET-receptor antagonism increases the CO and decreases the peripheral resistance in patients with congestive heart failure (71). On the contrary, C5a causes histamine release from mast cells, which may lead to enhanced vascular permeability and a relative blood loss into the dilated vessels. The

elevation in plasma histamine level in the early post-tamponade phase, together with previous data, shows that this level is higher in the portal venous blood than that in the arterial blood (14). In the presence of AcPepA, the histamine release was reduced, and this effect can also contribute to the increased venous return.

In this porcine model, the pericardial tamponade triggered characteristic macro- and microcirculatory changes in the bowels. The share of the splanchnic area from the reduced CO was diminished during the tamponade, but the SMA flow, which reflects the blood supply of the small intestine and colon, was restored thereafter, and no differences were observed compared to the sham-operated group. Nevertheless, in the AcPepA-treated group, the SMA flow was significantly elevated at the beginning of the post tamponade phase, and gradually returned to the control level by the end of the experiments. This early flow elevation may be attributable to the relative lack of vasoconstrictor ET-1 effects because it has been demonstrated that ET-A receptor inhibition is able to improve the splanchnic circulation in similar cases (25).

In shock conditions, an important feature of the splanchnic microcirculatory disturbances is heterogeneity, which worsens the oxygen supply and metabolism of the cells (72, 73). A heterogeneously oscillating microcirculation can be well characterized by the average RBCV (68, 74). It has been demonstrated that the duration of the high-flow component of a heterogeneous microcirculation is increased significantly following ET-A receptor inhibition (68). From this point of view, the excessive release of ET-1 can be an important part of the worsening of inflammatory responses, when intensive complement activation is present. ET-1 release can contribute to the impairment of the microcirculation and, due to its vasoconstrictor effects, to the changes in the macrohemodynamics throughout such conditions, and it can even influence the pattern of cytokine release (75).

The cause of the improved mucosal RBCV in the AcPepA-treated group may be multifactorial. The decreased levels of ET-1 formation and leukocyte activation each can effectively reduce the extent of intermediate reactive oxygen formation. By the reduction of these sources of tissue damage, the endothelial function can be preserved, which subsequently results in the improvement of microcirculation.

We found increased HMGB-1 levels after tamponade, which were significantly reduced by AcPepA treatment. These findings correlate to the similar results of continuous AcPepA treatment in a primate endotoxin shock model (50).

These results can be explained by the involvement of the C5L2 receptor, a high-affinity C5a receptor, which was earlier thought to be a non-signaling, scavenger receptor of C5a as it is incapable of G-protein coupling. Recent findings, however, have proved that C5L2 has a more important role in mediating inflammatory responses of the innate immune system. The survival rate in C5L2 knockout mice was increased after cecal ligation and puncture–induced sepsis in relation to the survival rate in wild-type mice and it has been described that the release of the potent proinflammatory cytokine HMGB-1 after endotoxin + C5a or only endotoxin administration was diminished in C5L2 knockout macrophages (45).

To determine the effects that can be linked to C5a antagonist treatment, we had to consider and rule out artificial influences that may originate from the experimental design. We, therefore, applied standard fluid replacement therapy in all groups to exclude the effects of the volume status on the microcirculation. The clinical limitations are evident, but it is very likely that a preserved microcirculatory function in the GI tract is mediated directly or indirectly by C5a pathways in this experimental NOMI model of anesthetized, ventilated, and thoracotomized minipigs.

In conclusion, these results demonstrated the emergence of NOMI among the acute circulatory complications of cardiac tamponade, and the potential role of C5a antagonism in reducing signals that are important components in the development of a secondary splanchnic microcirculatory disturbance.

5.2. Late hemodynamic and inflammatory consequences of NOMI in rats. Study II-III

We have designed an animal model in which the main clinical features of NOMI are reproducible. Key elements are persistently decreased SMA flow after an extramesenteric insult and the reduced invasiveness, which makes the long-term observations possible. In this context we have obtained conclusive evidences for the significantly diminished SMA blood flow after partial occlusion of the subdiaphragmatic aorta, which persisted during the 24 hour post-occlusion period, despite the compensated CO and MAP (see Table 2). It should be added that the late hemodynamic changes were characteristic to a systemic inflammatory response syndrome. Although MAP was in the normal range, the HR and CO was significantly increased, as part of the compensatory mechanism. During the early phase of systemic inflammation, the oxygen demand is increased due to the high metabolic rate. To

meet this need, oxygen delivery is increased mostly through the elevation of CO. Nevertheless, the oxygenation of the cells cannot be improved without a properly functioning microcirculation, and a deterioration of capillary perfusion will prevent the oxygen consumption despite the seemingly increased delivery. In our model the small intestinal microcirculation was significantly impaired 24 hours following the insult as shown by the decreased RBCV at both serosal and mucosal surfaces. This means that microcirculatory damage was present in the gastrointestinal wall despite of the normal or increased SMA flow (76).

Nevertheless, it is important to note some limitations of the experimental model. One of these is the significantly increased MAP that can evolve above the site of the aorta occlusion. It can approximate the upper limits of the cerebral autoregulation (77) for a short period, during the first 30 min of the PAO. However, the manoeuvre is tolerable, since no animals were lost during the first 24 hours and none of them showed any signs of injury of the central nervous system. The other problem is the need for invasive blood pressure measurement in the femoral artery because it provides more precise data for the adjustment of PAO as compared with the non-invasive possibilities. During the design of the model we took in consideration that well-developed collateral vascularization in the rat hind limb can provide adequate tissue perfusion even after the ligation of the femoral artery (78, 79). Nevertheless, before the recovery period, the animals were observed and in case of any signs of permanent hind limb ischemia, like cyanosis, stiffness, the experiment was terminated and the animals were excluded from the study. The low number of such animals (n=3) suggests that the ligation of the femoral artery could be possible in these studies.

In this setup we have administered AcPepA, a synthetic, antisense C5a inhibitor compound. In the AcPepA-treated group, the small intestinal RBCV was significantly higher on day 2, and the improved microcirculation was present without an increase in CO and SMA flow which may refer to the better efficacy of oxygen extraction.

The decreased ET-1 level after AcPepA treatment may have contributed to the improvement of the small intestinal microcirculation, and the altered proinflammatory cytokine profile may also refer to a reduced inflammatory activation as a consequence of C5a inhibitor therapy. ET-1 is one of the most important vasoconstrictive factors in the splanchnic microcirculation, and it has been shown that administration of selective ET-A receptor antagonist significantly improves the small intestinal microcirculation in lowflow conditions

(68). More importantly, the excessive release of ET-1 enhances leukocyte activation in the postcapillary venules of the small intestine (44) which may further increase the local tissue damage.

The increased circulatory HMGB-1 and TNF-α levels are another important features of our model, and these findings are in concordance with the clinical observations (80). High level of TNF-α can directly impair gastrointestinal epithelial tight junctions (81), thus a decreased level of TNF-α in the AcPepA-treated group may not only be a direct sign of the alleviated inflammatory cascade activation, but may be indirectly associated with the preservation of the barrier function. Similarly, an increased HMGB-1 output can amplify the inflammatory signals and a significant decrease in the HMGB-1 level may be the key sign of decreased systemic inflammatory response (82). HMGB-1 is a highly potent alarming signal originating from necrotic cells or actively released from immune cells, and it causes leukocyte recruitment and the release of other inflammatory cytokines (46). The release is directly mediated by C5a through C5L2 receptors and the blockade or absence of C5L2 receptors improves the survival in murine sepsis (45). The net result of a diminished HMGB-1 and TNF-α release is the reduced leukocyte accumulation. This was verified by traditional histology: leukocyte infiltration was significantly lower in the small intestinal wall in the AcPepA-treated group. All these macro-, microcirculatory and inflammatory effects of PAO culminated in visible damage of the mucosa (see Figure 5), and C5a inhibition that resulted in a significant decrease in tissue damage, preserved villus structure and microvascular architecture was demonstrated by *in vivo* histology as well.

In summary, we have characterized some of the potentially detrimental circulatory and proinflammatory consequences of non-occlusive mesenteric hypoperfusion in a novel rodent model. In this experimental setup, a single *iv* dose of complement C5a antagonist AcPepA compound was suitable for improving the local circulatory changes and it reduced the secondary mucosal damage in a relatively wide time frame, at least 24 hours after the insult. The human relevance of these data is still unknown, but the approach holds promise for future use in NOMI-associated situations.

6. SUMMARY OF NEW FINDINGS

- Experimental pericardial tamponade causes systemic inflammation and diminished microcirculation in the splanchnic area, and this provides opportunity to study the pathophysiology of NOMI in a large animal model.

- Complement C5a antagonist treatment with AcPepA improves the splanchnic microcirculation and reduces the acute inflammatory consequences of pericardial tamponade, thus complement activation can play a role in the short-term microcirculatory disturbances of NOMI.

- We have developed and characterized a new rodent model of partial aorta occlusion, and adapted it to the investigation of the long-term hemodynamic and inflammatory consequences of experimental NOMI in a clinically relevant time frame.

- Experimental NOMI diminishes the microcirculation within the intestinal wall and causes inflammatory activation and secondary mucosal damage. The complement C5a antagonist AcPepA treatment is competent to improve the microcirculation and reduces the inflammatory activation, which suggests that complement activation plays a central role also in the late, potentially damaging consequences of NOMI.

8. REFERENCES

1. Acosta S: Epidemiology of Mesenteric Vascular Disease: Clinical Implications. *Semin Vasc Surg* 2010; 23:4–8

2. Dahlke MH, Asshoff L, Popp FC, et al.: Mesenteric ischemia--outcome after surgical therapy in 83 patients. *Dig Surg* 2008; 25:213–219

3. van den Heijkant TC, Aerts BA, Teijink JA, et al.: Challenges in diagnosing mesenteric ischemia. *World J Gastroenterol WJG* 2013; 19:1338–1341

4. SUN Y, GAO Q, WU N, et al.: Protective effects of dexmedetomidine on intestinal ischemia-reperfusion injury. *Exp Ther Med* 2015; 10:647–652

5. Toung T, Reilly PM, Fuh KC, et al.: Mesenteric vasoconstriction in response to hemorrhagic shock. *Shock Augusta Ga* 2000; 13:267–273

6. Muschitz GK, Fochtmann A, Keck M, et al.: Non-occlusive mesenteric ischaemia: the prevalent cause of gastrointestinal infarction in patients with severe burn injuries. *Injury* 2015; 46:124–130

7. Tsuji Y, Kodama Y, Chiba T, et al.: Severe acute pancreatitis and non occlusive mesenteric ischemia. *Nippon Fukubu Kyukyu Igakkai Zasshi* 2011; 31:1029–1037

8. Goleanu V, Alecu L, Lazar O: Acute mesenteric ischemia after heart surgery. *Chir Buchar Rom 1990* 2014; 109:402–406

9. Trompeter M, Brazda T, Remy CT, et al.: Non-occlusive mesenteric ischemia: etiology, diagnosis, and interventional therapy. *Eur Radiol* 2002; 12:1179–1187

10. Björck M, Wanhainen A: Nonocclusive mesenteric hypoperfusion syndromes: recognition and treatment. *Semin Vasc Surg* 2010; 23:54–64

11. Klar E, Rahmanian PB, Bücker A, et al.: Acute mesenteric ischemia: a vascular emergency. *Dtsch Ärztebl Int* 2012; 109:249–256

12. Schoots IG, Koffeman GI, Legemate DA, et al.: Systematic review of survival after acute mesenteric ischaemia according to disease aetiology. *Br J Surg* 2004; 91:17–27

13. Seferović PM, Ristić AD, Imazio M, et al.: Management strategies in pericardial emergencies. *Herz* 2006; 31:891–900

14. Kaszaki J, Nagy S, Tárnoky K, et al.: Humoral changes in shock induced by cardiac tamponade. *Circ Shock* 1989; 29:143–153

15. Bailey RW, Bulkley GB, Hamilton SR, et al.: The fundamental hemodynamic mechanism underlying gastric "stress ulceration" in cardiogenic shock. *Ann Surg* 1987; 205:597–612

16. Buerke M, Lemm H, Dietz S, et al.: Pathophysiology, diagnosis, and treatment of infarction-related cardiogenic shock. *Herz* 2011; 36:73–83

17. Williams RA, Wilson SE: A model for the study of nonocclusive intestinal ischaemia. *Br J Exp Pathol* 1980; 61:461–464

18. Weitzberg E, Ahlborg G, Lundberg JM: Long-lasting vasoconstriction and efficient regional extraction of endothelin-1 in human splanchnic and renal tissues. *Biochem Biophys Res Commun* 1991; 180:1298–1303

19. Oldner A, Wanecek M, Goiny M, et al.: The endothelin receptor antagonist bosentan restores gut oxygen delivery and reverses intestinal mucosal acidosis in porcine endotoxin shock. *Gut* 1998; 42:696–702

20. Boros M, Szalay L, Kaszaki J: Endothelin-1 induces mucosal mast cell degranulation and tissue injury via ETA receptors. *Clin Sci Lond Engl 1979* 2002; 103 Suppl 48:31–34

21. Scaffidi P, Misteli T, Bianchi ME: Release of chromatin protein HMGB1 by necrotic cells triggers inflammation. *Nature* 2002; 418:191–195

22. Kaszaki J, Wolfárd A, Szalay L, et al.: Pathophysiology of Ischemia-Reperfusion Injury. *Transplant Proc* 2006; 38:826–828

23. Soop A, Albert J, Weitzberg E, et al.: Complement activation, endothelin-1 and neuropeptide Y in relation to the cardiovascular response to endotoxin-induced systemic inflammation in healthy volunteers. *Acta Anaesthesiol Scand* 2004; 48:74–81

24. Yasue N, Guth PH: Role of exogenous acid and retransfusion in hemorrhagic shock-induced gastric lesions in the rat. *Gastroenterology* 1988; 94:1135–1143

25. Wolfárd A, Vangel R, Szalay L, et al.: Endothelin-A receptor antagonism improves small bowel graft perfusion and structure after ischemia and reperfusion. *Transplantation* 1999; 68:1231–1238

26. Boros M, Kaszaki J, Nagy S: Histamine release during intestinal ischemia-reperfusion: role of iron ions and hydrogen peroxide. *Circ Shock* 1991; 35:174–180

27. Boros M, Karácsony G, Kaszaki J, et al.: Reperfusion mucosal damage after complete intestinal ischemia in the dog: the effects of antioxidant and phospholipase A2 inhibitor therapy. *Surgery* 1993; 113:184–191

28. Carter MB, Wilson MA, Wead WB, et al.: Platelet-activating factor mediates pulmonary macromolecular leak following intestinal ischemia-reperfusion. *J Surg Res* 1996; 60:403–408

29. Kaszaki J, Boros M, Szabó A, et al.: Role of histamine in the intestinal flow response following mesenteric ischemia. *Shock Augusta Ga* 1994; 2:413–420

30. Yao YM, Sheng ZY, Yu Y, et al.: The potential etiologic role of tumor necrosis factor in mediating multiple organ dysfunction in rats following intestinal ischemia-reperfusion injury. *Resuscitation* 1995; 29:157–168

31. Tamion F, Richard V, Lyoumi S, et al.: Gut ischemia and mesenteric synthesis of inflammatory cytokines after hemorrhagic or endotoxic shock. *Am J Physiol* 1997; 273:G314–321

32. Riedemann NC, Ward PA: Complement in Ischemia Reperfusion Injury. *Am J Pathol* 2003; 162:363–367

33. Charles A Janeway J, Travers P, Walport M, et al.: The complement system and innate immunity [Internet]. 2001; [cited 5 July 2016] Available at: http://www.ncbi.nlm.nih.gov/books/NBK27100/

34. Sarma JV, Ward PA: The Complement System. *Cell Tissue Res* 2011; 343:227–235

35. Granger CB, Mahaffey KW, Weaver WD, et al.: Pexelizumab, an anti-C5 complement antibody, as adjunctive therapy to primary percutaneous coronary intervention in acute myocardial infarction: the COMplement inhibition in Myocardial infarction treated with Angioplasty (COMMA) trial. *Circulation* 2003; 108:1184–1190

36. Ehrengruber MU, Geiser T, Deranleau DA: Activation of human neutrophils by C3a and C5A. Comparison of the effects on shape changes, chemotaxis, secretion, and respiratory burst. *FEBS Lett* 1994; 346:181–184

37. Sacks T, Moldow CF, Craddock PR, et al.: Oxygen radicals mediate endothelial cell damage by complement-stimulated granulocytes. An in vitro model of immune vascular damage. *J Clin Invest* 1978; 61:1161–1167

38. Zimmermann T, Laszik Z, Nagy S, et al.: The role of the complement system in the pathogenesis of multiple organ failure in shock. *Prog Clin Biol Res* 1989; 308:291–297

39. Ember JA, Sanderson SD, Hugli TE, et al.: Induction of interleukin-8 synthesis from monocytes by human C5a anaphylatoxin. *Am J Pathol* 1994; 144:393–403

40. Mollnes TE, Brekke O-L, Fung M, et al.: Essential role of the C5a receptor in E coli-induced oxidative burst and phagocytosis revealed by a novel lepirudin-based human whole blood model of inflammation. *Blood* 2002; 100:1869–1877

41. Okada N, Asai S, Hotta A, et al.: Increased inhibitory capacity of an anti-C5a complementary peptide following acetylation of N-terminal alanine. *Microbiol Immunol* 2007; 51:439–443

42. Lemaire LC, van Lanschot JJ, Stoutenbeek CP, et al.: Bacterial translocation in multiple organ failure: cause or epiphenomenon still unproven. *Br J Surg* 1997; 84:1340–1350

43. Zhang X, Kimura Y, Fang C, et al.: Regulation of Toll-like receptor-mediated inflammatory response by complement in vivo. *Blood* 2007; 110:228–236

44. Boros M, Massberg S, Baranyi L, et al.: Endothelin 1 induces leukocyte adhesion in submucosal venules of the rat small intestine. *Gastroenterology* 1998; 114:103–114

45. Rittirsch D, Flierl MA, Nadeau BA, et al.: Functional roles for C5a receptors in sepsis. *Nat Med* 2008; 14:551–557

46. Ulloa L, Messmer D: High-mobility group box 1 (HMGB1) protein: friend and foe. *Cytokine Growth Factor Rev* 2006; 17:189–201

47. Haynes DR, Harkin DG, Bignold LP, et al.: Inhibition of C5a-induced neutrophil chemotaxis and macrophage cytokine production in vitro by a new C5a receptor antagonist. *Biochem Pharmacol* 2000; 60:729–733

48. Lee H, Whitfeld PL, Mackay CR: Receptors for complement C5a. The importance of C5aR and the enigmatic role of C5L2. *Immunol Cell Biol* 2008; 86:153–160

49. Fujita E, Farkas I, Campbell W, et al.: Inactivation of C5a anaphylatoxin by a peptide that is complementary to a region of C5a. *J Immunol (Baltim Md 1950)* 2004; 172:6382–6387

50. Okada H, Imai M, Ono F, et al.: Novel complementary peptides to target molecules. *Anticancer Res* 2011; 31:2511–2516

51. Erces D, Nógrády M, Nagy E, et al.: Complement C5A Antagonist Treatment Improves the Acute Circulatory and Inflammatory Consequences of Experimental Cardiac Tamponade. *Crit Care Med* 2013; 41(11):e344-51

52. Kozuch PL, Brandt LJ: Review article: diagnosis and management of mesenteric ischaemia with an emphasis on pharmacotherapy. *Aliment Pharmacol Ther* 2005; 21:201–215

53. Kang H, Manasia A, Rajamani S, et al.: Intravenous iloprost increases mesenteric blood flow in experimental acute nonocclusive mesenteric ischemia. *Crit Care Med* 2002; 30:2528–2534

54. Bailey RW, Bulkley GB, Hamilton SR, et al.: Protection of the small intestine from nonocclusive mesenteric ischemic injury due to cardiogenic shock. *Am J Surg* 1987; 153:108–116

55. MacCannell KL, Newton CA, Lederis K, et al.: Use of selective mesenteric vasodilator peptides in experimental nonocclusive mesenteric ischemia in the dog. *Gastroenterology* 1986; 90:669–676

56. Starr FL, Samphilipo MA, White RI, et al.: A reproducible canine model of nonocclusive mesenteric ischemia. *Invest Radiol* 1982; 17:34–36

57. MacCannell KL: Comparison of an intravenous selective mesenteric vasodilator with intraarterial papaverine in experimental nonocclusive mesenteric ischemia. *Gastroenterology* 1986; 91:79–83

58. Åneman A, Treggiari MM, Burgener D, et al.: Tezosentan normalizes hepatomesenteric perfusion in a porcine model of cardiac tamponade. *Acta Anaesthesiol Scand* 2009; 53:203–209

59. Pindiprolu P, Epner M, Berger A, et al.: Efficacy of the porcine model for demonstrating pericardial effusion with real-time ultrasound. *Acad Emerg Med Off J Soc Acad Emerg Med* 2000; 7:1169

60. Terajima K, Aneman A, Haljamäe H: Haemodynamic effects of volume resuscitation by hypertonic saline-dextran (HSD) in porcine acute cardiac tamponade. *Acta Anaesthesiol Scand* 2004; 48:46–54

61. Zhang H, Vincent JL: Oxygen extraction is altered by endotoxin during tamponade-induced stagnant hypoxia in the dog. *Circ Shock* 1993; 40:168–176

62. Zhang H, Spapen H, Benlabed M, et al.: Systemic oxygen extraction can be improved during repeated episodes of cardiac tamponade. *J Crit Care* 1993; 8:93–99

63. Di Segni E, Feinberg MS, Sheinowitz M, et al.: Left ventricular pseudohypertrophy in cardiac tamponade: an echocardiographic study in a canine model. *J Am Coll Cardiol* 1993; 21:1286–1294

64. Davis JW, McKone TK, Cram AE: Hemodynamic effects of military anti-shock trousers (MAST) in experimental cardiac tamponade. *Ann Emerg Med* 1981; 10:185–186

65. Picard MH, Sanfilippo AJ, Newell JB, et al.: Quantitative relation between increased intrapericardial pressure and Doppler flow velocities during experimental cardiac tamponade. *J Am Coll Cardiol* 1991; 18:234–242

66. Kuebler WM, Abels C, Schuerer L, et al.: Measurement of neutrophil content in brain and lung tissue by a modified myeloperoxidase assay. *Int J Microcirc Clin Exp Spons Eur Soc Microcirc* 1996; 16:89–97

67. Zimmermann T, Schuster R, Lauschke G, et al.: Chemiluminescence response of whole blood and separated blood cells in cases of experimentally induced pancreatitis and MDTQ-DA—Trasylol—ascorbic acid therapy. *Anal Chim Acta* 1991; 255:373–381

68. Szabó A, Suki B, Csonka E, et al.: Flow motion in the intestinal villi during hemorrhagic shock: a new method to characterize the microcirculatory changes. *Shock Augusta Ga* 2004; 21:320–328

69. Malle E, Furtmüller PG, Sattler W, et al.: Myeloperoxidase: a target for new drug development? *Br J Pharmacol* 2007; 152:838–854

70. Vollmar B, Menger MD: Intestinal ischemia/reperfusion: microcirculatory pathology and functional consequences. *Langenbecks Arch Surg Dtsch Ges Für Chir* 2011; 396:13–29

71. Lüscher TF, Barton M: Endothelins and endothelin receptor antagonists: therapeutic considerations for a novel class of cardiovascular drugs. *Circulation* 2000; 102:2434–2440

72. Ince C: The microcirculation is the motor of sepsis. *Crit Care Lond Engl* 2005; 9 Suppl 4:13–19

73. De Backer D, Ortiz JA, Salgado D: Coupling microcirculation to systemic hemodynamics. *Curr Opin Crit Care* 2010; 16:250–254

74. Vajda K, Szabó A, Boros M: Heterogeneous microcirculation in the rat small intestine during hemorrhagic shock: quantification of the effects of hypertonic-hyperoncotic resuscitation. *Eur Surg Res Eur Chir Forsch Rech Chir Eur* 2004; 36:338–344

75. Matsushima H, Yamada N, Matsue H, et al.: The effects of endothelin-1 on degranulation, cytokine, and growth factor production by skin-derived mast cells. *Eur J Immunol* 2004; 34:1910–1919

76. Tao W, Zwischenberger JB, Nguyen TT, et al.: Gut mucosal ischemia during normothermic cardiopulmonary bypass results from blood flow redistribution and increased oxygen demand. *J Thorac Cardiovasc Surg* 1995; 110:819–828

77. Paulson OB, Strandgaard S, Edvinsson L: Cerebral autoregulation. *Cerebrovasc Brain Metab Rev* 1990; 2:161–192

78. Brevetti LS, Paek R, Brady SE, et al.: Exercise-induced hyperemia unmasks regional blood flow deficit in experimental hindlimb ischemia. *J Surg Res* 2001; 98:21–26

79. Hellingman AA, Bastiaansen AJNM, de Vries MR, et al.: Variations in surgical procedures for hind limb ischaemia mouse models result in differences in collateral formation. *Eur J Vasc Endovasc Surg Off J Eur Soc Vasc Surg* 2010; 40:796–803

80. Cremer J, Martin M, Redl H, et al.: Systemic inflammatory response syndrome after cardiac operations. *Ann Thorac Surg* 1996; 61:1714–1720

81. Shen L, Turner JR: Role of epithelial cells in initiation and propagation of intestinal inflammation. Eliminating the static: tight junction dynamics exposed. *Am J Physiol Gastrointest Liver Physiol* 2006; 290:G577–582

82. Wang H, Bloom O, Zhang M, et al.: HMG-1 as a late mediator of endotoxin lethality in mice. *Science* 1999; 285:248–251

9. ACKNOWLEDGEMENTS

I would like to express my gratitude to Professor Mihály Boros, head of Institute of Surgical Research, for his scientific guidance. I greatly appreciate the encouragement and support he has given me through the years, during which I have had the possibility to work in his department.

I am especially grateful to my supervisors, Gabriella Varga and Dániel Érces for their personal guidance and for introducing me to experimental surgery. Their guidance helped me in all the time of research and writing of this thesis. I could not have imagined having a better advisor and mentor for my Ph.D study.

I express my thanks for the excellent technical assistance of the Institute of Surgical Research and for József Kaszaki, who was my first supervisor at the begining of my research work as a student.

My sincere thanks also goes to Gábor Németh, head of Department of Obstetrics and Gynecology, who provided me the opportunity to do my research near my clinical work.

I am also grateful to my supervisor in clinical researches, Andrea Surányi, for her enormous help and for her valuable suggestions that contributed to the improvement of the scientific value of the studies included in this PhD thesis.